



**MARYLAND DEPARTMENT OF
TRANSPORTATION STATE HIGHWAY
ADMINISTRATION**

RESEARCH REPORT

**OFF-LINE AND REAL-TIME EVALUATIONS
OF EASTERN-SHORE SENSORS WITH A
GENERALIZED DETECTION PERFORMANCE
MONITORING SYSTEM**

**YI-TING LIN, YEN-HSIANG CHEN, YEN-LIN
HUANG, YAO CHENG, GANG-LEN CHANG**

**THE UNIVERSITY OF MARYLAND,
COLLEGE PARK**

FINAL REPORT

March 2023

This material is based on work supported by the Federal Highway Administration under the State Planning and Research program. Any opinions, findings, and conclusions or recommendations expressed in this publication are those of the author(s) and do not necessarily reflect the views of the Federal Highway Administration or the Maryland Department of Transportation. This report does not constitute a standard, specification, or regulation.

TECHNICAL REPORT DOCUMENTATION PAGE

1. Report No.	2. Government Accession No.	3. Recipient's Catalog No.	
4. Title and Subtitle Off-Line and Real-Time Evaluations of Eastern-Shore Sensors with a Generalized Detection Performance Monitoring System		5. Report Date October 1, 2022	
		6. Performing Organization Code	
7. Author(s) Yi-Ting Lin, Yen-Hsiang Chen, Yen-Lin Huang, Yao Cheng, Gang-Len Chang		8. Performing Organization Report No.	
9. Performing Organization Name and Address The University of Maryland, College Park, MD 20742		10. Work Unit No.	
		11. Contract or Grant No. SHA/UM/6-8	
12. Sponsoring Agency Name and Address Maryland Department of Transportation (SPR) State Highway Administration Office of Policy & Research 707 North Calvert Street Baltimore MD 21202		13. Type of Report and Period Covered SPR-B Final Report (June 2012-June 2014*) *This is the performing period.	
		14. Sponsoring Agency Code (7120) STMD - MDOT/SHA	
15. Supplementary Notes			
16. Abstract The primary objectives of this study are to develop a detector performance monitoring system for both off-line and on-line applications, and to implement such a system for the Eastern Shore region's current and proposed sensors, including: evaluate the data quality and reliability of the six sensors deployed in the Eastern Shore region; assess the applicability of the six sensors in the Eastern Shore region for supporting various traffic monitoring and congestion-control strategies; and analyze the data applicability and effectiveness of the proposed 14 more sensors for the Eastern Shore region for traffic monitoring, congestion control, or emergency evaluation, based on their proposed deployment locations. The first product of this study is a set of guidelines for selecting the deployment locations for traffic sensors in the Eastern Shore region for different purposes, such as speed monitoring, signal design, or congestion control. The second product is an innovative, multi-stage control model for traffic professionals to efficiently assess the quality of massive speed and flow rate data produced from a deployed detector. Based on the quality assessment results, the responsible maintenance engineers/staff can better classify the operational status of each deployed detector, including "for speed-monitoring only," "for traffic control and management," "need to replace with new detector," and "need a field calibration to improve the detection accuracy."			
17. Key Words detector assessment, multi-stage, data quality control		18. Distribution Statement This document is available from the Research Division upon request.	
19. Security Classif. (of this report) None	20. Security Classif. (of this page) None	21. No. of Pages	22. Price

Table of Contents

Table of Contents	iv
List of Figures.....	v
List of Tables	viii
Chapter 1. Introduction	1
1.1 Research Background.....	1
1.2 Research Objective	1
1.3 Report Organization	2
Chapter 2. Evaluation and Calibration of Radar-based Traffic Detector	4
2.1 Introduction	4
2.2 Detector Accuracy Evaluation.....	4
2.3 Procedures for Detector Calibration	7
2.4 Summary of Research Findings.....	11
Chapter 3: Assessing the Data Quality of Radar-based Highway Traffic Sensors.....	13
3.1 Background.....	13
3.2 Data Quality Assessment for Radar-based Traffic Sensors.....	14
3.3 System Operation and Development	26
3.4 System Application with the Customized Software	33
Chapter 4: Selection of Locations for Eastern Shore Sensor Deployment.....	42
4.1 Introduction	42
4.2 Method for Selecting Detector Deployment Locations	42
4.3 List of Locations Recommended for Detector Deployments in the Eastern Shore Region	47
4.4 Summary Findings.....	62
Chapter 5: Conclusion and Recommendations.....	64
5.1 Conclusion of Research Findings	64
5.2 Potential Extensions	65
References	67
Appendices.....	70
Appendix-A	70
Appendix-B	71

List of Figures

Figure 2-1: The video image of a highway segment taken by a drone for evaluating a target detector’s measurement accuracy	5
Figure 2-2: Example of geo-registration to match the target roadway segment in the drone’s video with its real-world coordinates.....	5
Figure 2-3: Illustration of setting the measurement points on the target roadway segment.....	6
Figure 2-4: Example of setting a measurement gate at the target detector’s location from a drone’s video image.....	6
Figure 2-5: Example of interface pages for volume adjustment with the detector-specific calibration software.....	8
Figure 2-6: Example of interface pages for speed adjustment with the detector-specific calibration software (Wavetronix LLC, 2015).....	9
Figure 2-7: Example of aligning the direction of the target detector’s radar wave from the calibration software.....	10
Figure 2-8: Example of aligning the zone coverage of the target detector’s radar wave from the calibration software.....	10
Figure 2-9: Example of aligning the angle and height of the target detector’s radar wave from the calibration software.....	11
Figure 2-10: Illustration of the zone coverage by a side-fire detector’s radar waves (RTMS training manual, 2006)	11
Figure 3-1: Fundamental diagram of the speed and flow-rate relationship from sensor 317 (between 08/17/2018 and 09/15/2018) on the Eastern Shore, MD.....	17
Figure 3-2: Graphical illustration of Stage 2A test, using the zone-based control for data quality assessment with the data from sensor 317	19
Figure 3-3: Graphical illustration of speed flow data classified into three distinct traffic states	22
Figure 3-4: Temporal patterns for the Eastern Shore region’s touring traffic detected by for sensor 317 (09/03/2018)	25
Figure 3-5: The operational flowchart for the entire system	27
Figure 3-6: Illustrating the bagplot results from Zone 3 for constructing the boundaries.....	28
Figure 3-7: Boundaries identification for Zone 1	30
Figure 3-8: Identification of the transition zone	31
Figure 3-9: Development of speed-flow relationship for oversaturated traffic state (Mean Error: 2.12 vphpl)	32
Figure 3-10: Development of speed-flow relationship for undersaturated traffic state during peak hours	33
Figure 3-11: Log in to RITIS to download the sensor data of interest	34

Figure 3-12: Interface of the developed software for data quality assessment.....	34
Figure 3-13: Interface page for uploading the target detector’s file	35
Figure 3-14: Interface page for summary of information associated with the uploaded file.....	35
Figure 3-15: Interface page to show the assessment results	36
Figure 3-16: Interface page to download the analysis result details of interest.....	36
Figure 3-17: Graphical illustration of the speed-flow relationships from three well-calibrated sensors.....	38
Figure 3-18: Graphical illustration of the speed-flow relationships from three not-calibrated sensors.....	39
Figure 3-19: An example of Stage 2C test based on sensor 301 (09/03/2018).....	41
Figure 4-1: Graphical illustration of the decomposed congestion patterns within the Eastern Shore region.....	44
Figure 4-2: Example of the speed-evolution data for identifying and decomposing congestion patterns.....	44
Figure 4-3: Results of congestion pattern analysis for Cluster 1 congested highway segment within the Eastern Shore region.....	45
Figure 4-4: Detector locations selected for different application needs	46
Figure 4-5: The list of recommended locations and available infrastructure for detector deployment for Cluster 1 congested highway segment in the Eastern Shore region.....	47
Figure 4-6: Results of congestion pattern analysis for Cluster 2 congested highway segment in the Eastern-shore region	49
Figure 4-7: The list of recommended locations and available infrastructure for detector deployment for Cluster 2 congested highway segment in the Eastern Shore region.....	50
Figure 4-8: Results of congestion pattern analysis for Cluster 3 congested highway segment in the Eastern Shore region	52
Figure 4-9: List of results of congestion pattern analysis for Cluster 3 congested highway segment in the Eastern Shore region.....	53
Figure 4-10: Examples of detector deployment for monitoring turning traffic volumes at major intersections	54
Figure 4-11: Results of congestion pattern analysis for Cluster 4 congested highway segment in the Eastern Shore region	55
Figure 4-12: Geometric features of the two congested intersections and suggested locations for detector deployment.....	55
Figure 4-13: List of detectors recommended for Cluster 4 congested highway segment in the Eastern Shore region.....	56
Figure 4-14: geometric features of the two locations (C16 and C17) for detector placement....	57
Figure 4-15: List of detectors recommended for Cluster 5 congested highway segment in the Eastern Shore region.....	58

Figure 4-16: List of detectors recommended for Cluster 6 congested highway segment in the Eastern Shore region	59
Figure 4-17: Results of congestion pattern analysis for Cluster 7 congested highway segment in the Eastern Shore region	60
Figure 4-18: List of detectors recommended for Cluster 7 congested highway segment in the Eastern Shore region	61
Figure 4-19: List of detectors recommended for Cluster 8 congested highway segment over Bay Bridge	62
Figure A-1: An example of the downloaded analysis results from the developed software	70
Figure B-1: Lane configuration Sensor S122001	73
Figure B-2: Lane configuration Sensor S122002	73
Figure B-3: Lane configuration Sensor S217004	74
Figure B-4: Lane configuration Sensor S217002	74
Figure B-5: Lane configuration Sensor S217003	75
Figure B-6: Lane configuration Sensor S110002	75
Figure B-7: Lane configuration Sensor S110001	76
Figure B-8: Lane configuration Sensor S110003	76

List of Tables

Table 2-1: Example of the evaluation results for a detector’s measurement accuracy.....	7
Table 2-2: Definitions for all variables used to compute SQV.....	8
Table 3-1: Mathematical expressions for the boundaries of the four screening zones with data from sensor 317.....	20
Table 3-2: Calibrated upper and lower bounds for the Stage-2B test.....	23
Table 3-3: Test the saturation level during each time period.....	26
Table 3-4: Results of trend consistency test for small intervals in Period 2.....	26
Table 3-4: Evaluation results of well-calibrated sensors	37
Table 3-5: Screening results of low-quality sensors	37
Table 3-6: Examples of Stage 2C test results	40
Table 4-1 Summary of detector locations recommended for Eastern Shore deployment.	63
Table B-1: Evaluation results of sensor accuracy.....	72

Chapter 1. Introduction

1.1 Research Background

MDOT SHA has recently installed six Wavetronix sensors on the Eastern Shore, with plans to deploy an additional 14 sensors on scheduled dates. The six Wavetronix sensors, installed on June 8 and 9, 2022, operate in real-time to provide traffic data for use in CHART ATMS and for traffic professionals via the RITIS platform. A rigorous quality evaluation with respect to the six existing sensors is essential to ensure the best application of their real-time data, and also for the review of the deployment plan for the remaining 14 sensors. The objective of a detector performance evaluation is to address the following issues:

- stability, availability, and the variance of time-series sensor data;
- accuracy and precision levels for flow rate, speed, and occupancy by lane;
- consistency of data accuracy under different congestion levels and various traffic compositions (e.g., percentage of heavy vehicles); and
- data applicability for different traffic control strategies based on their deployed locations.

It is expected that the results of such an evaluation task will produce sufficient information for developing an operational guide to optimize the remaining deployment of 14 sensors in the Eastern Shore region and for future sensor deployments across the state.

Beyond ensuring the data quality for the Eastern Shore sensors, assessing their potential effectiveness to support various traffic control and management strategies is also an imperative task. The result of such an assessment will help the responsible engineers finalize the location selection for the proposed 14 sensors and estimate if additional sensors are needed to manage the Eastern Shore region's peak-period congestion or support emergency evacuation during the hurricane season.

1.2 Research Objective

The primary objectives of this study are to develop a detector performance monitoring system for both off-line and on-line applications, and to implement such a system for the Eastern Shore region's current and proposed sensors, including:

- evaluate the data quality and reliability of the six sensors deployed in the Eastern Shore region;

- assess the applicability of the six sensors in the Eastern Shore region for supporting various traffic monitoring and congestion-control strategies; and
- analyze the data applicability and effectiveness of the proposed 14 more sensors for the Eastern Shore region for traffic monitoring, congestion control, or emergency evaluation, based on their proposed deployment locations.

1.3 Report Organization

All research results and primary findings from this study are organized into five chapters and presented in this report. A brief description of the primary tasks and information contained in each chapter is summarized below:

Chapter 2 describes the drone-based data collection method for assessing the accuracy of traffic measurements produced by typical radar-based detectors. Compared to the use of road-side camcorders, which record traffic images and then measure the volume and speed off line, the digitized video images from a standing drone can concurrently measure the flow rate and speed by lane over the target roadway segment at a high level of accuracy.

A step-by-step description of the calibration process for radar-based detectors is also included in this chapter based on the information available from the calibration manual for Wavetronix sensors, a standard radar-based highway traffic detector. Since all commercial radar-based traffic detectors in the traffic engineering market share the same design logic and key system features, one can certainly apply the same procedures for calibrating other brands of radar-based traffic detectors.

Chapter 3 presents the review results of literature associated with detector quality evaluation, including statistical algorithms or software available for both off-line and on-line assessment. The review efforts have focused on identifying any state-of-the-art tools or methods for responsible engineers/staffs to conveniently assess the healthy state of a target set of detectors over a selected time period and produce recommendations, such as “need accuracy calibration,” “need maintenance,” and “need replacement.”

The description of a customized, multi-stage assessment algorithm for detector quality comprises the core of this chapter. The phase-1 functions and output provided by the assessment algorithm is presented first, focusing on its off-line analysis process for assessing a target detector’s data availability, reliability, and quality. This is followed by an in-depth discussion of traffic flow properties during peak and off-peak periods, and the logic of converting such fundamental properties to an innovative quality control system for a target traffic sensor’s data accuracy. Application results of the developed detector quality assessment algorithm have also been included in this chapter.

Chapter 4 reports the assessment results with respect to 20 proposed locations for deploying traffic sensors on the Eastern Shore, focusing on their individual and collective effectiveness for traffic controls, congestion management, and emergency evacuation. This chapter begins with a concise illustration of the multi-stage process for assessing the effectiveness of a target detector's traffic data for intended applications, followed by its implementation for assessing each candidate detector location, based on the evolution of congestion patterns, distribution of traffic volume in the detection zone, and available spatial coverage of potential bottlenecks. A list of locations recommended for deployment of a comprehensive traffic monitoring system within the Eastern Shore region is also included in this chapter.

Chapter 5 presents the key research findings from this study, including the developed software and user guide. Future work that forwards the study's findings to manage recurrent congestion on the Eastern Shore is also provided in this chapter.

Chapter 2. Evaluation and Calibration of Radar-based Traffic

Detectors

2.1 Introduction

The process for determining if a target highway detector needs to be recalibrated or replaced generally consists of the following two stages:

- Stage 1: Compare the accuracy of traffic measurements (i.e., speed, flow rate, and occupancy) provided by the target detector with the ground-truth data using reliable methods (e.g., drone or roadside video recording).
- Stage 2: If the quality of traffic measurements and the data availability are within the acceptable range, perform field calibration to improve the detector's accuracy level, using the software provided by its manufacturer.

Note that a detector shall be replaced if it cannot be calibrated to reliably measure the target spot's traffic conditions, especially the flow rate and speed. A brief discussion of activities performed at the evaluation stage with a drone-based method is presented in the next section. This is followed by a step-by-step description of the key steps conducted at the calibration stage in section 2-3. Concluding comments and main findings are summarized in the last section.

2.2 Detector Accuracy Evaluation

To evaluate a detector's measurement accuracy, one can compute the ground-truth data from video images recorded by roadside camcorders or an unmanned aircraft (i.e., drone). Since the latter can reliably provide the speed of each vehicle over the target roadway zone covered by the target detector, its resulting measurements can concurrently produce the total volume over the observed period and the speed distribution of observed vehicles for effective comparison with the same information from the target detector. Figure 2-1 shows the image of a roadway traffic zone taken by a drone for detector accuracy evaluation. Table 2-1 presents an example of comparison results between measurements by the target detector and the same information measured from the drone's recorded images.

A concise description of the keys steps to produce such traffic measurements with a drone is summarized below:

Perform traffic measurements with a drone

Step 1: Deploy the drone at a fixed location and record the images and activities of the

roadway segment covered by the target traffic detector, as shown in Figure 2-1.



Figure 2-1: The video image of a highway segment taken by a drone for evaluating a target detector’s measurement accuracy

Step 2: Conduct the geo-registration to match the target roadway segment in the drone’s video with its real-world coordinates (see Figure 2-2).



Figure 2-2: Example of geo-registration to match the target roadway segment in the drone’s video with its real-world coordinates

Step 3: Measure the distance between two pre-specified points in the video from the target roadway segment to ensure that the geo-registration is done properly; if not, go to Step 2.



Figure 2-3: Illustration of setting the measurement points on the target roadway segment

Step 4: Set a measurement gate at the location of the target detector to count vehicles passing through the gate and measure their speeds.

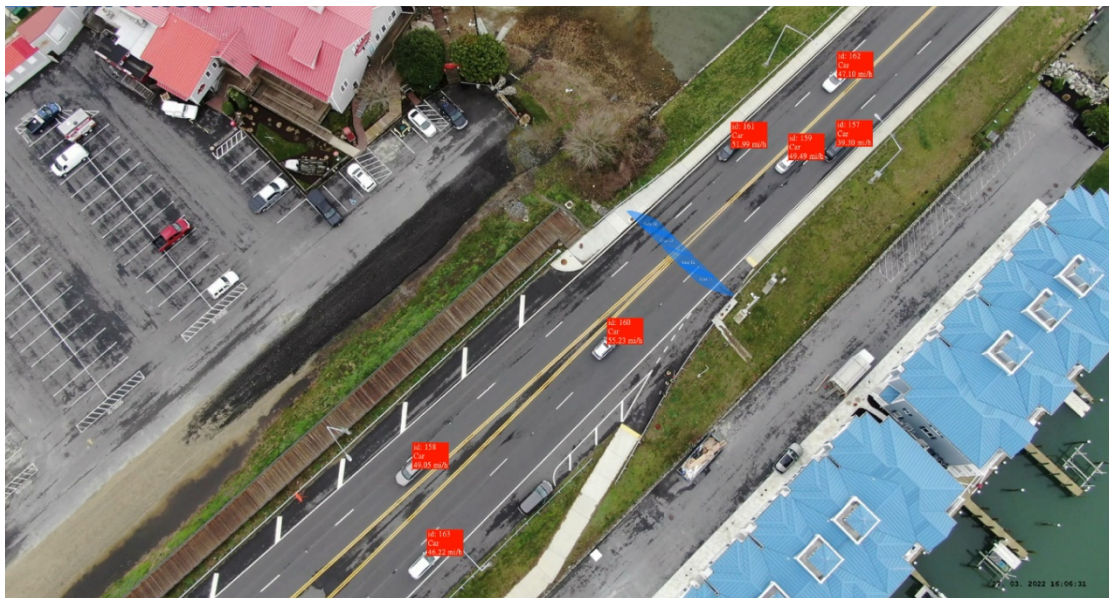


Figure 2-4: Example of setting a measurement gate at the target detector's location from a drone's video image

Step 5: Compare the measurements of speeds and flowrates by drone with those by the detector.

Table 2-1 shows an example of comparison results between the data by the done and the detector at the location shown in Figure 2-1. Note that the volume data for Lane 3, as shown in the table, differ more than 10% from the ground-truth results, indicating that this target detector’s overall quality is not acceptable, and needs calibration work to ensure that the radar beams emitted from the detector can cover the entire lane and catch all passing vehicles.

Table 2-1: Example of the evaluation results for a detector’s measurement accuracy

	Volume (1 min)	Volume (15 min)	Volume (1 hour)	Speed (1 min)	Speed (15 min)	Speed (1 hour)
Lane 1	4.6%	0.6%	0.0%	1.2%	0.5%	0.4%
Lane 2	4.2%	1.8%	1.7%	1.1%	0.8%	0.2%
Lane 3	18.9%	12.5%	12.3%	1.6%	0.4%	0.1%
Lane 4	4.4%	2.8%	1.6%	1.5%	0.4%	0.2%

2.3 Procedures for Detector Calibration

Note that the detector calibration task will be essential if the field evaluation results show that the target detector can consistently produce the measurement data but not up to the required level of accuracy. Since all manufacturers for commercial radar-based detectors generally provide customized software for calibration of their own products, one can perform such a task with the following typical steps:

Step 1: Select a target period for field collection of the ground-truth traffic volume and speed data over the roadway segment covered by the target detector.

Step 2: Perform the following statistic indicator, SQV (Scalable Quality Value) by Friedrich et al. (2019) to compare the volume data produced by the target detector with the measured ground-truth data:

$$SQV = \frac{1}{1 + \sqrt{\frac{(q_{t,l} - \hat{q}_{t,l})^2}{f \cdot q_{t,l}}}} \quad (2-1)$$

The definitions for all variables in Equation 2-1 are shown in the following table:

Table 2-2: Definitions for all variables used to compute SQV

Notation	Definition
$q_{t,l}$	Ground-truth speed at interval t , lane l
$v_{t,l}$	Ground-truth volume at interval t , lane l
$\hat{q}_{t,l}$	Measured speed by the detector at interval t , lane l
$\hat{v}_{t,l}$	Measured volume by the detector at interval t , lane l
N	Number of sample intervals over the entire field observation period
f	Parameter for computing SQV based on the volume data

Step 3: Proceed to Step 7 for speed calibration if all SQVs over the observation period equal or are larger than 0.90 to confirm that the volume data from the detector is sufficiently accurate; otherwise, go to next step.

Step 4: Perform the on-site connection (or via remote connection by the control center) between the customized calibration software and the target detector if most SQVs are below 0.90 and $\hat{q}_{t,l}$ differs systematically from the $q_{t,l}$ over most intervals.

Step-5: Adjust the target detector for volume detection from the software's interface (see Figure 2-5), by either tuning up the volume percentage or through less attenuation (dB<0, dB>0) if the detected volume is less than the ground-truth value.

Step 6: Continue the adjustment with Step 5 until the detector-produced volumes are statistically indifferent from the ground truth data and then proceed to the speed calibration.

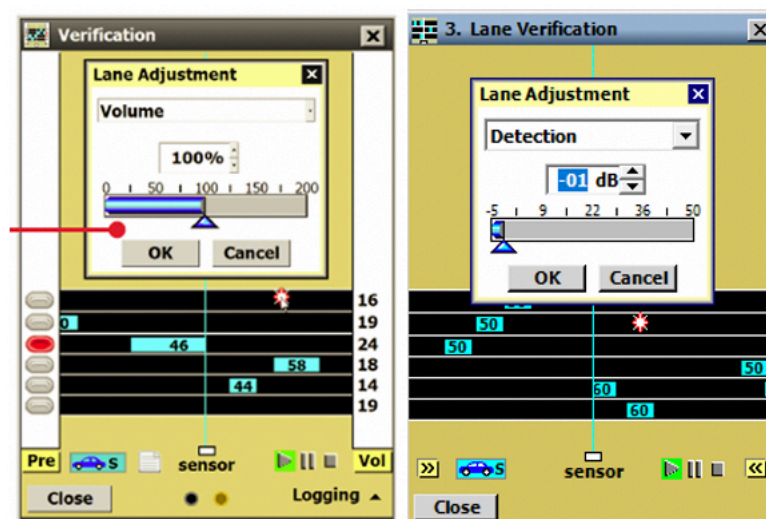


Figure 2-5: Example of interface pages for volume adjustment with the detector-specific calibration software

Step 7: perform the speed calibration by first computing the following MAE:

$$\text{Speed MAPE (lane } l) = \sum_t |v_{t,l} - \hat{v}_{t,l}| / (Nv_{t,l}) \quad (2-2)$$

If the MAE is sufficiently small (e.g., 5%), one can conclude that the speed data measured by the target detector are sufficiently reliable, and then terminate the calibration task; otherwise, proceed to next step.

Step 8: Conduct the paired t-test (REF) between the set of speed data from the detector and the ground-truth data; if these two sets of data exhibit a statistically significant difference, proceed to the next step for speed adjustment with the calibration software.

Step 9: Connect the sensor to the calibration software (same as for volume calibration), and tune up (down) the “speed” cursor on the interface (see Figure 2-6) if the detected speeds are less than (higher) the ground-truth speeds.

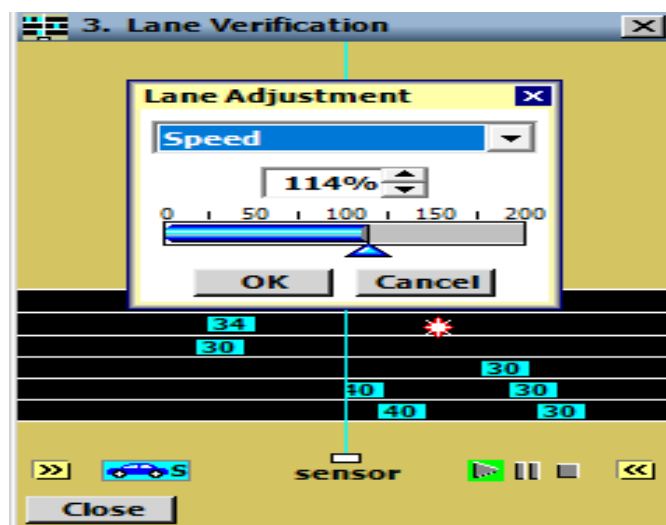


Figure 2-6: Example of interface pages for speed adjustment with the detector-specific calibration software (Wavetronix LLC, 2015)

Additional steps for detector realignment

Note that if executing Step 6 and Step 9 cannot calibrate the detector’s volume and speed measurements to the acceptable level of accuracy, one will need to first realign the mounted detector’s vision angle (see Step 10) with the following steps and then re-execute steps 1 to 9.

Step 10: Adjust the detector’s vision direction to ensure that it is perfectly perpendicular to target roadway, as shown in Figure 2-7.

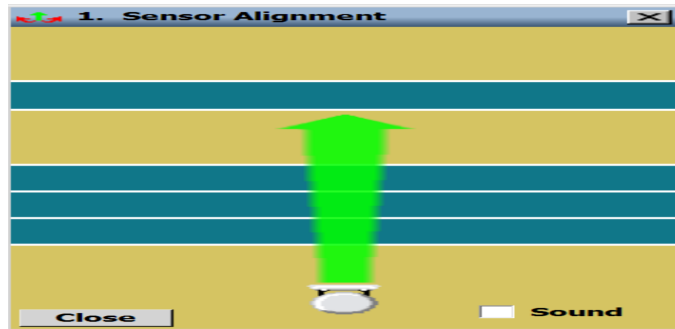


Figure 2-7: Example of aligning the direction of the target detector’s radar wave from the calibration software

Step 11: Use the calibration software’s interface (see Figure 2-8) to adjust the coverage of the radar waves (e.g., adjusting the lane width or lane position) until all travel lanes are displayed properly on the screen.

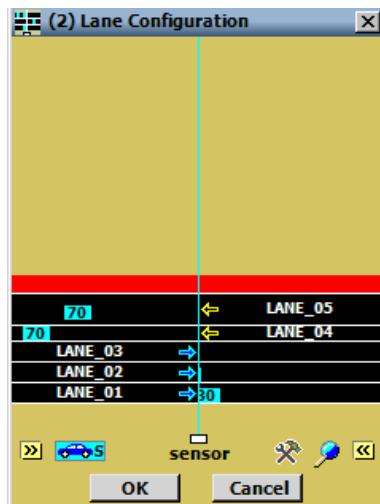


Figure 2-8: Example of aligning the zone coverage of the target detector’s radar wave from the calibration software

Step 12: Verify if vehicles on all travel lanes are captured properly and shown on the screen of the calibration software; otherwise, adjust the sensor’s angle or height, as shown in Figure 2-9, until there is no interference by any nearby objects (e.g., guardrail).

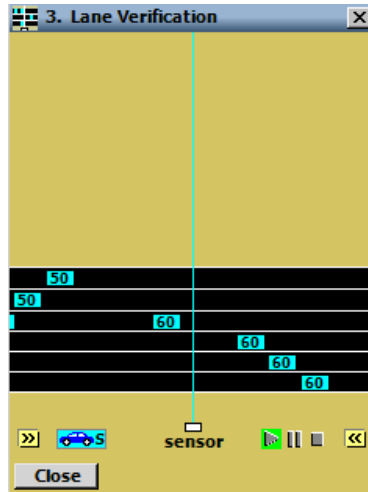


Figure 2-9: Example of aligning the angle and height of the target detector’s radar wave from the calibration software

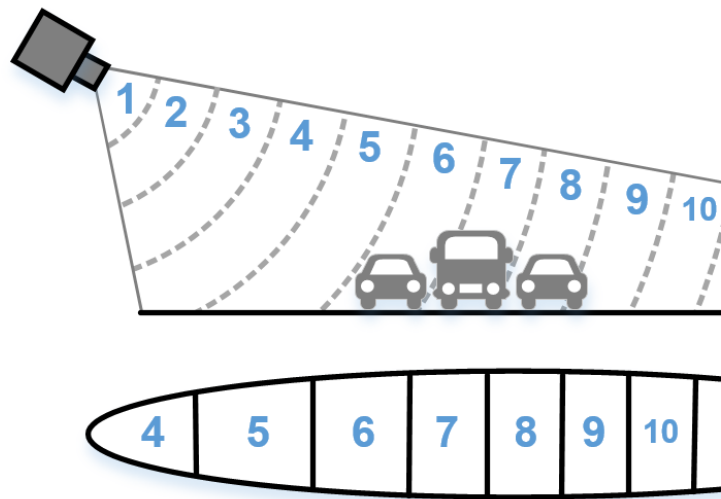


Figure 2-10: Illustration of the zone coverage by a side-fire detector’s radar waves (RTMS training manual, 2006)

Note that all existing radar-based traffic detectors are typically mounted on the roadside of the target highway segment. Figure 2-10 illustrates the spatial distribution of the emitted radar wave zones, which should be calibrated with steps 10-12 to precisely map each travel lane to one or an integer number of zones so that vehicles over such travel lanes will not be missed or double-counted.

2.4 Summary of Research Findings

This chapter has described the drone-based data collection method for assessing the accuracy of traffic measurements produced by typical radar-based detectors. Different from

the use of roadside camcorders, which record the traffic images and then measure the volume and speed off-line, the digitized video images from a standing drone can concurrently measure the flow rate and speed by lane over the target roadway segment at a high-level of accuracy. Since new drone technologies can provide a high-precision image at a relative low cost, traffic engineers may consider taking advantage of such advancements for both detector quality assessment and other traffic data collection.

As for the detector calibration process, all procedures discussed in this chapter are based on the information available from the calibration manual for Wavetronix sensors, a standard radar-based highway traffic detector. Since all commercial radar-based traffic detectors in the traffic engineering market share the same design logic and key system features, one can certainly apply the same procedures for calibrating other brands of radar-based traffic detectors.

Note that the presented calibration process does not include occupancy, one of the key traffic measurements provided by most types of traffic detectors. This is due mainly to the fact that the occupancy data by Wavetronix sensors (and other similar type of sensors) do not actually produced from field measurements, but apply an empirical formula converted from the speed and vehicle length (Wavetronix LLC, 2018). In addition, the collection of occupancy data for calibration needs will require a set of special devices and extended efforts to perform the field measurement work at the desirable level of accuracy. From both traffic control and management perspectives, one can comfortably view a detector as producing quality data if its measurements of speed and flow rate are sufficiently reliable and accurate.

Chapter 3: Assessing the Data Quality of Radar-based Highway Traffic Sensors

3.1 Background

From day-to-day congestion monitoring to the design of real-time or time-of-day traffic control strategies, most control centers often face the challenge of how to effectively assess the quality of data from deployed sensors. Such data (i.e., speed, flow rate, and occupancy), either from conventional loop detectors or roadside-mounted radar sensors, are typically produced in real-time and at intervals of shorter than 30 seconds (prior to any aggregation). As such, the amount of data from a highway system's traffic detectors, even archived only over a short operational period (e.g., one month), could render the quality assessment work prohibitively time-consuming and difficult if without a reliable and efficient tool.

Because most highway control centers mainly rely on information from extensively deployed sensors to monitor traffic conditions and implement control strategies, the development of an effective tool to identify sensors of unreliable quality in a timely manner has emerged as an imperative task in the traffic community.

In a review of related literature associated with detector data quality assessment, one can classify all state-of-the-art and state-of-the-practice methods for such needs into the following categories: basic validity tests to flag data errors and advanced detection algorithms to identify faulty or low-quality data. Most tests in the former category apply pre-calibrated thresholds for a single variable (e.g., occupancy) or multivariate (e.g., speed and occupancy) quality analysis, enabling the quality evaluation process to rule out the obvious abnormal data without going through complex computing procedures (Cleghorn et al., 1991; Turochy and Smith, 2000; Turner et al., 2000; Weijermars and Berkum, 2006; Smith and Venkatanarayana, 2007; Chen et al., 2019; Azin and Yang, 2020). Such tests are often viewed as the first essential task for further assessment of a detector's data quality.

Most algorithms proposed in the literature that further identify a detector's faulty or low-quality data share one or more of the following features: (1) assessment of the fundamental traffic flow relations (e.g., volume, occupancy) revealed from the data; (2) consistency comparison of key traffic flow characteristics between detectors in the neighboring lanes; and (3) spatial correlation of traffic patterns between two closely spaced detectors. For example, grounded on the results of extensive data analyses, some studies proposed the use of a calibrated feasible region for the volume-occupancy ratio under various traffic states and locations as the set of thresholds for faulty or low-quality data detection (Jacobson et al., 1990; Nihan, 1990; Cleghorn et al., 1991; Chen et al., 2003; Al-Deek et al., 2004).

With the same notion of applying the feasible relations among fundamental traffic flow properties for data quality assessment, traffic researchers over the past two decades developed various statistical methods for detecting faulty data, based on the statistical consistency of average effective vehicle length (AEVL) computed over the same time period by detectors in adjacent lanes or at nearby upstream/downstream locations (Turochy and Smith, 2000; Ametha et al., 2001; Wang et al., 2009; Lu et al., 2014; Zefreh and Torok 2018, Azin and Yang, 2020; Ariannezhad and Wu, 2020). Note that the notion of comparing the AEVL or key traffic flow variables for data quality assessment has been used for both single loop and dual loops (Wall and Dailey, 2003; Weijermars and Berkum, 2006; Chen and May, 1987; Coifman, 1999; Wang et al., 2009). Some researchers have further advanced the off-line detection algorithms for real-time identification of malfunctioning detectors with advanced statistical methods (e.g., Peeta and Anastassopoulos, 2002; Ishak et al., 2007; Wu et al., 2010; Corey et al., 2011; Ghafouri et al., 2017). A comprehensive review of most such detection methods is available in the work by Chen et al. (2019).

It should be noted that all aforementioned detection algorithms, despite their significant contributions, have been developed mainly for loop detectors, where the occupancy data plays a key role in deriving AEVL or for checking the consistency between key traffic flow properties measured from different loops for comparison. The increasingly popular radar-based traffic detector, as discussed previously, does not directly measure occupancy, but derives such information from the relations between speed, flow rate, and vehicle length. Hence, for data quality assessment of existing side-fired radar detectors, this study has proposed an effective two-stage evaluation model, focusing mainly on the speed and flow data and their relationships.

3.2 Data Quality Assessment for Radar-based Traffic Sensors

This chapter presents a two-stage process for data quality assessment of radar-based traffic sensors. The first stage is designed mainly for assessing the detector's missing data rate and the percentage of faulty data, called the validity test (Chen et al., 2019). The second stage, comprising three sequential tests, functions to assess if those data, passing through Stage 1 screening, have the quality consistent with traffic flow theory and daily traffic dynamics in either saturated or undersaturated conditions.

Note that data quality assessment for radar-based traffic sensors focuses mainly on produced speeds and flow rates, but not occupancy. This is because, unlike loop-based detectors, traffic sensors using side-fired radar waves do not directly measure the occupancy but compute such information from detected flow rates and speeds (Wavetronix LLC. 2018-Documentation 0299). In addition, the actual roadway segment covered by a roadside-

mounted radar sensor varies from lane to lane, depending on various factors such as the height of its vision, angle, and the number of travel lanes on the target roadway segment. The resulting discrepancy in the spatial coverage on each lane by the radar waves from the same side-mounted sensor directly contributes to the difficulty of measuring occupancy at the desirable level of accuracy.

Stage 1: Computing the percentage of missing and faulty data

Any method available in the preliminary quality control literature for detecting missing and faulty data is applicable at this stage. The study has adopted the following steps to perform the target detector's data screening:

- **Step 1:** Download the speed and flow rate data (per unit interval of 30 seconds or one minute) produced by the target traffic sensor over the time period of interest (e.g., one month).
- **Step 2:** Select two critical thresholds (TH1, and TH2) for making the following assessment decision.
- **Step 3:** If data availability is less than TH1 (e.g., 75%), then the sensor should be replaced; if data availability is greater than TH2 (e.g., 95%) then proceed to the validity test of faulty data; if data availability is between TH1 and TH2, then proceed to Step 4.
- **Step 4:** Conduct pattern analysis for the missing data.

Note that the primary focus of the Step 4 analysis is to identify if any systematic data-missing patterns in the archived dataset are attributable to factors that have been removed or no longer exist. Under such scenarios, one can then remove those missing-data intervals from the original dataset and reconduct the same screening process. In contrast, if the missing data intervals are randomly distributed over the entire period of interest due to unidentifiable factors, then this detector should be removed for maintenance.

Note that in executing the above steps, one should preset the thresholds of TH1 and TH2 based on the purpose of using the target traffic sensor's data. Conceivably, such thresholds for real-time traffic control should be much higher than those mainly for traffic congestion monitoring.

Detection of faulty data

For detector data passing through the availability screening, the next step is to identify any obvious faulty data with the following criteria:

- during peak hours of congested days, their flow rates cannot exceed the historical upper bound of q_{cp}^u vphpl, or be lower than the historical lower bound of q_{cp}^l vphpl;
- during off-peak hours of congested days, their flow rates cannot exceed the historical upper bound of q_{co}^u vphpl;
- during peak hours of non-congested days, the flow rates cannot exceed the historical threshold of q_{np}^u vphpl;
- during off-peak hours of non-congested days, their flow rates cannot exceed the historical threshold of q_{no}^u vphpl;
- during peak hours, either congested or non-congested days, their speeds cannot exceed the historical threshold of u_{ub} mph; and
- during incident-free off-peak hours, either congested or non-congested days, their speeds cannot be lower than the historical threshold of u_{lb} mph.

Note that one can compute the control bounds or thresholds for the above screening criteria with any basic quality control method (e.g., 99% confidence interval), using available historical data generated by a high-quality detector from the same region or highway network. Also note that all speed and flow data—as long as it is distributed within their theoretically or historically feasible ranges—can pass through the above validity tests. Hence, one needs to further assess the quality of such data with the speed-flow relations exhibited under different traffic conditions.

Stage 2: Evaluation of a detector's data quality

The focus at this stage is to further assess the quality of the speed-flow data passing through Stage 1 screening assessment with three sequential tests, based on the expected traffic-flow relationships under various traffic conditions. The proposed Stage 2 tests are grounded in the extensive speed-flow data from a healthy and well-calibrated traffic detector (see Figure 3-1), which shall exhibit the following distinct characteristics:

- Much of such speed-flow data at the aggregated level (e.g., per minute interval over one month) will scatter around the fundamental diagram demonstrating their theoretical relationship (see Figure 3-2). Their distributions may vary with the location-specific factors, including behaviors of the driving population, congestion level, roadway geometric features, weather, and environmental conditions, as well as deployed control strategies.
- The actual flow rate corresponding to a field detected speed often distributes within a range where its upper and lower bounds vary with the traffic conditions, such as peak

or off-peak periods, and saturated or undersaturated states.

- At the time-of-day temporal level, both the speed and flow rate from a healthy detector tends to move in the same direction (i.e., increase or decrease) during saturated or oversaturated states; such a relationship does not hold, and can even show the opposite trend, if traffic conditions are evolving in the undersaturated state.

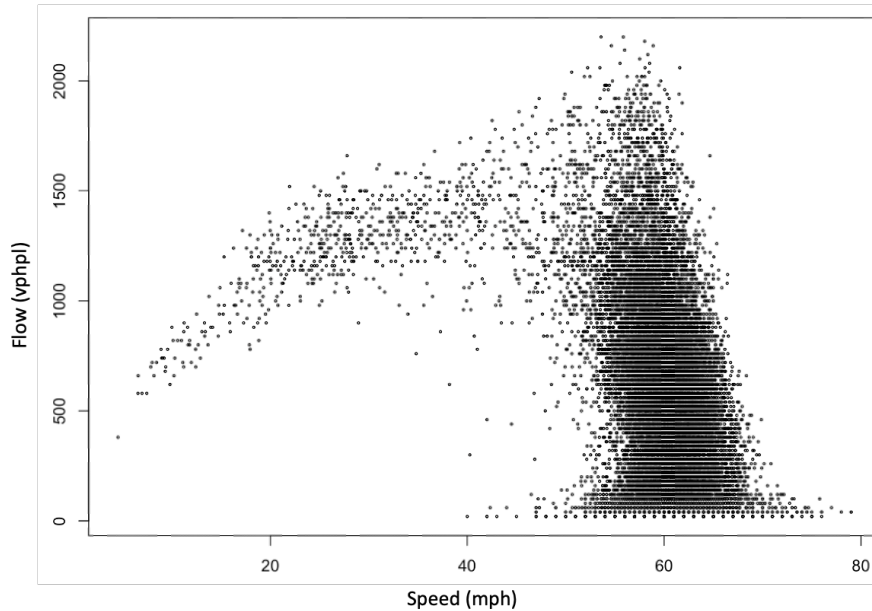


Figure 3-1: Fundamental diagram of the speed and flow-rate relationship from sensor 317 (between 08/17/2018 and 09/15/2018) on the Eastern Shore, MD.

With the above understanding of speed-flow relationships from both the traffic flow theory and empirical observations, this study has proposed the following three consecutive tests for detector data quality:

Stage 2A test: This is a zone-based screening test, proposed under the assumption that all pairs of speed-flow data, irrespective of the aggregation interval, should distribute around the theoretical fundamental diagram, as shown in Figure 3-2, if the data are from a well-calibrated traffic detector. Such well-distributed speed-flow data can generally be grouped into several distinct clusters, each encircled by a set of best-calibrated boundaries to ensure their total inclusion of 95% or more data points.

Figure 3-2 shows the distribution of speed-flow data from a well-calibrated traffic sensor (i.e., sensor 317 from the Eastern Shore, MD), with the four clusters optimally generated with the K-mean cluster method (Macqueen, 1967) to best group them. Hence, by mathematically specifying the boundaries for those four zones to include the target percentage of data, one can then use such zones to perform the data quality screening for other detectors in the same traffic system. The algorithm developed for identifying such boundaries will be discussed in

the later section. An example of such zone boundaries for use in screening other detectors' data is shown in Table 3-1, where any pair of speed-flow data not within any of these zones shall be classified as not having acceptable quality.

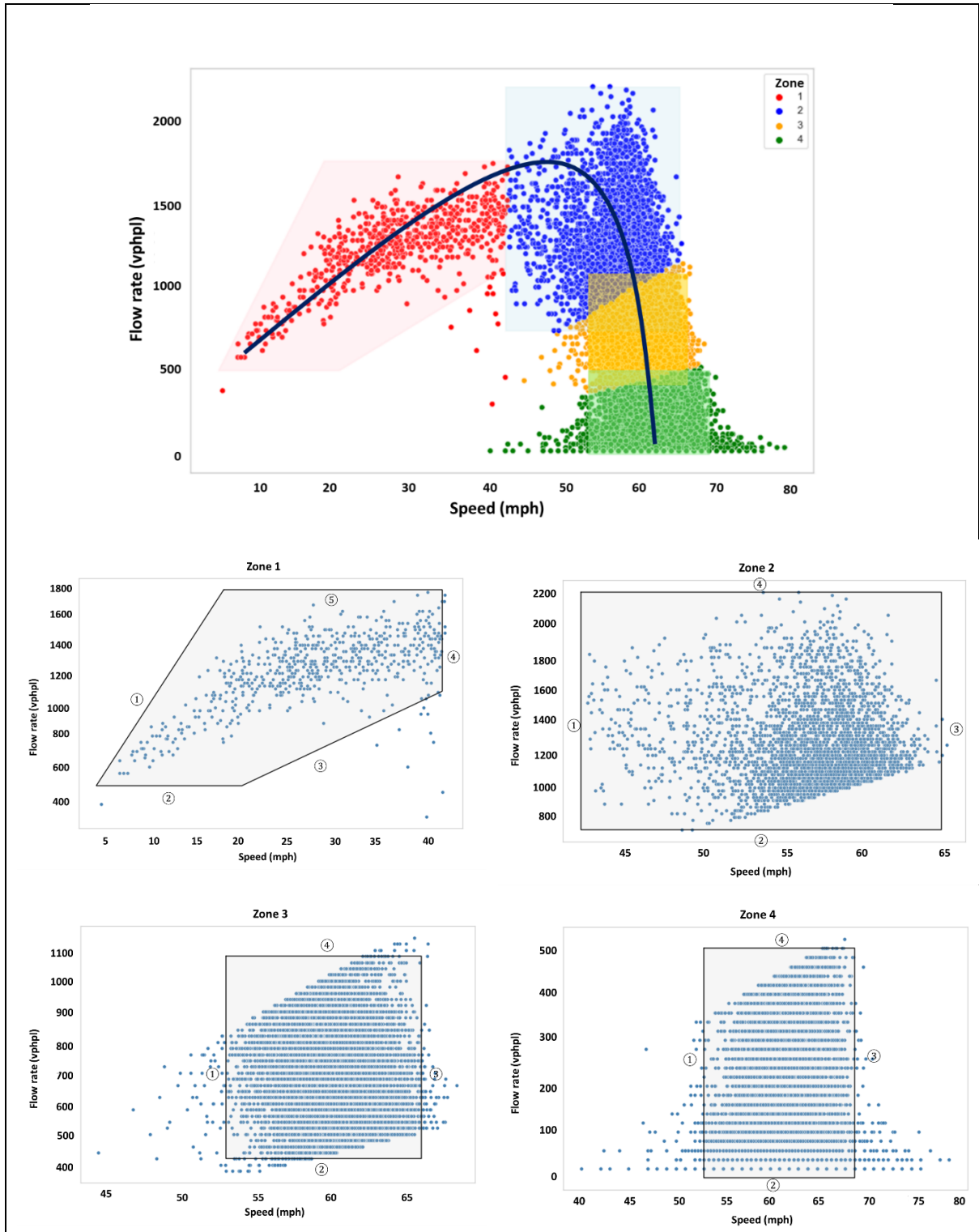


Figure 3-2: Graphical illustration of Stage 2A test, using the zone-based control for data quality assessment with the data from sensor 317

Table 3-1: Mathematical expressions for the boundaries of the four screening zones with data from sensor 317

Zone	Boundaries of the zone	Coverage of the zone
1	$f_1^1(x) = 90x + 142$ ($4 \leq x \leq 18$; $500 \leq y \leq 1755$)	$(f_1^1(x) - y \geq 0) \cap$
	$f_2^1(x) = 500$ ($4 \leq x \leq 20$)	$(f_2^1(x) - y \leq 0) \cap$
	$f_3^1(x) = 28x - 50$ ($20 \leq x \leq 42$; $500 \leq x \leq 1105$)	$(f_3^1(x) - y \leq 0) \cap$
	$f_4^1(y) = 42$ ($1105 \leq y \leq 1755$)	$(f_4^1(y) - x \geq 0) \cap$
	$f_5^1(x) = 1755$ ($18 \leq x \leq 42$)	$(f_5^1(x) - y \geq 0)$
2	$f_1^2(y) = 42$ ($740 \leq y \leq 2200$)	$(f_1^2(y) - x \leq 0) \cap$
	$f_2^2(x) = 740$ ($42 \leq x \leq 65$)	$(f_2^2(x) - y \leq 0) \cap$
	$f_3^2(y) = 65$ ($740 \leq y \leq 2200$)	$(f_3^2(y) - x \geq 0) \cap$
	$f_4^2(x) = 2200$ ($42 \leq x \leq 65$)	$(f_4^2(x) - y \geq 0)$
3	$f_1^3(y) = 53$ ($420 \leq y \leq 1080$)	$(f_1^3(y) - x \leq 0) \cap$
	$f_2^3(x) = 420$ ($53 \leq x \leq 66$)	$(f_2^3(x) - y \leq 0) \cap$
	$f_3^3(y) = 66$ ($420 \leq y \leq 1080$)	$(f_3^3(y) - x \geq 0) \cap$
	$f_4^3(x) = 1080$ ($53 \leq x \leq 66$)	$(f_4^3(x) - y \geq 0)$
4	$f_1^4(y) = 53$ ($0 \leq y \leq 500$)	$(f_1^4(y) - x \leq 0) \cap$
	$f_2^4(x) = 0$ ($53 \leq x \leq 69$)	$(f_2^4(x) - y \leq 0) \cap$
	$f_3^4(y) = 69$ ($0 \leq y \leq 500$)	$(f_3^4(y) - x \geq 0) \cap$
	$f_4^4(x) = 500$ ($53 \leq x \leq 69$)	$(f_4^4(x) - y \geq 0)$

Note: f_j^i denotes the j^{th} function of i^{th} zone, x denotes the recorded speed (mph), and y denotes the recorded flow rate (veh/hr).

Stage 2B test: This test is developed in recognition of the fact that a range of flow rates in the traffic stream, depending on the saturation level, may correspond to the same speed level (after removing the data noise). Such a variation range, however, may vary from undersaturated to oversaturated traffic conditions. Hence, one can employ such feasible ranges of flow variation, if well calibrated, at a given speed under different saturation levels to further assess the quality of those speed-flow data passing through the zone-base screening test.

Figure 3-3 further highlights different saturation levels in the speed-flow distribution pattern where traffic data are classified into the following three clusters: oversaturated, undersaturated, and transition states:

- **Cluster 1:** Comprise all speed-flow data points during the saturated or oversaturated traffic conditions.
- **Cluster 2:** Include detector data recorded for traffic conditions under transition

between saturated and undersaturated states.

- **Cluster 3:** Record all speed-flow data during the undersaturated traffic state, either during peak or off-peak periods.

Note that one can further divide the undersaturated traffic states into peak and off-peak periods if the data are sufficient. Also, such traffic state-dependent patterns clearly reveal that an accurately recorded speed data point may correspond to a range of traffic flow rates due to behavioral discrepancies among driving populations and different compositions of vehicles in the traffic flows. Hence, by rigorously calibrating such variation ranges for flow rates under different traffic states from a field-validated detector, one can further use such information to evaluate the quality of the speed-flow data from other detectors deployed over the same highway. This is one more step of quality assessment with respect to those data passing through the zone-based quality screening, to account for potential variation between the speed-flow relationships in real-world traffic flows under different saturation states.

Table 3-2 lists all such calibrated boundaries for the flow rate variation under different traffic states; the employed calibration algorithms are discussed in the next section.

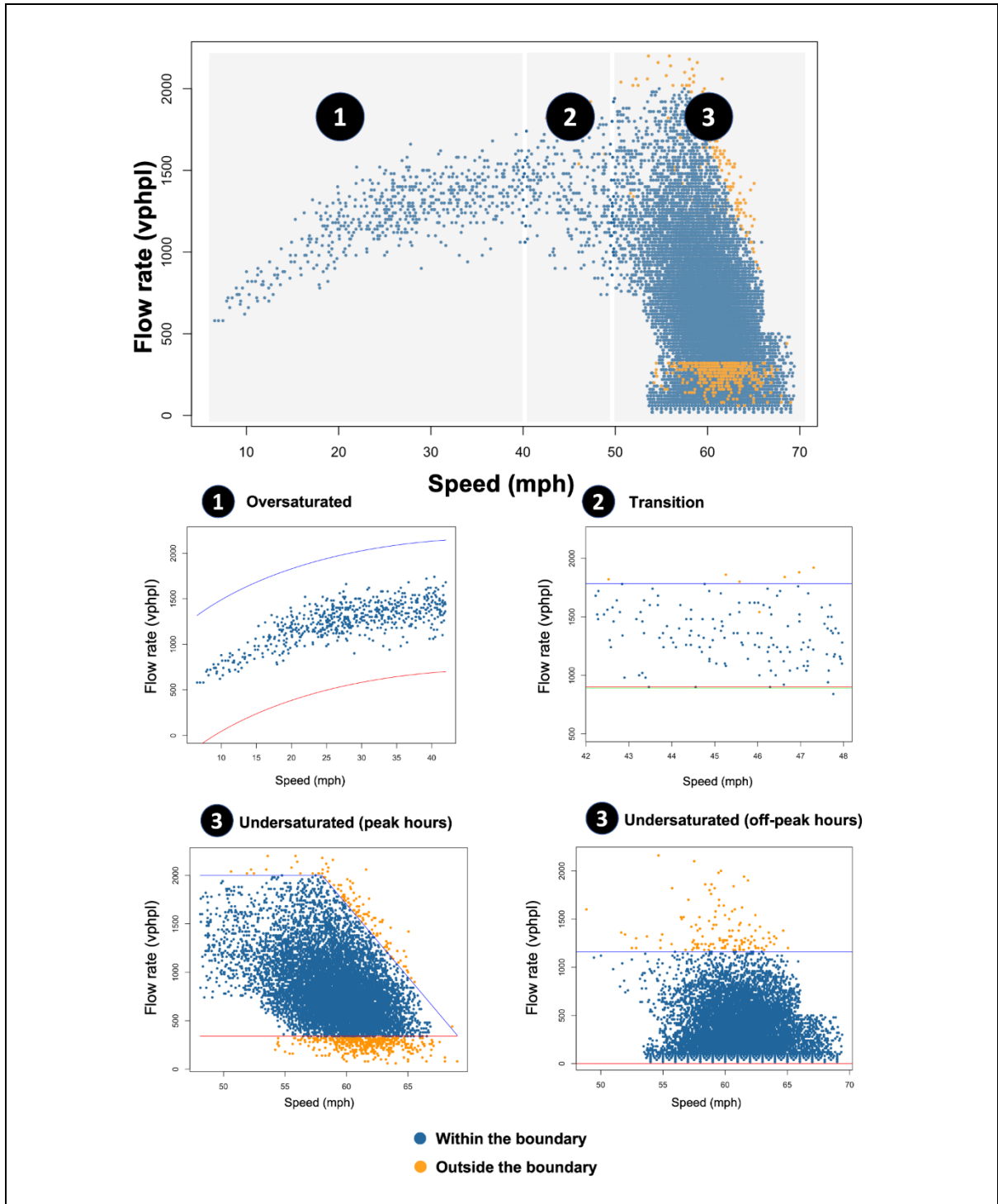


Figure 3-3: Graphical illustration of speed flow data classified into three distinct traffic states

Table 3-2: Calibrated upper and lower bounds for the Stage 2B test

Traffic state	Potential upper and lower bounds for flow rate (vphpl)
Saturated/Oversaturated $v < 40$ mph	$\begin{cases} q^{upper} = 2.44 \times v \times \ln \left(\left(\frac{2v_0}{v} \right)^{\frac{1}{0.09}} - 1 \right) + 368.34 \\ q^{lower} = 2.44 \times v \times \ln \left(\left(\frac{2v_0}{v} \right)^{\frac{1}{0.09}} - 1 \right) - 368.34 \end{cases}$
Undersaturated ($v > 50$ mph) Peak hours Off – peak hours	$\begin{cases} q^{upper} = \min \left(C, 200 + (v_0 - v) \times \left(\frac{C - 200}{v_0 - 58} \right) \right) \\ q^{lower} = 500 \\ \begin{cases} q^{upper} = 1160 \\ q^{lower} = 0 \end{cases} \end{cases}$
Transition state $40 \leq v \leq 50$ mph	$\begin{cases} q^{upper} = 1800 \\ q^{lower} = 900 \end{cases}$

Note: v and v_0 denote the recorded and free-flow speed, respectively; C denotes the capacity per lane; q^{upper} and q^{lower} denote the upper and lower bounds of the flow rate per lane, respectively

Stage 2C test: It is designed to further assess the data quality under different daily saturation levels where the temporal mutual relationship between the speed and flow rate will be evaluated to ensure that they are trending in the right direction during different time periods of a day. This temporal quality test is grounded in the following understanding of traffic flow characteristics:

- Traffic conditions, reflected in the detected speed-flow data over a typical day (see Figure 3-4) can be classified into multiple time periods of distinctly different states; the traffic conditions in each time period are likely in either a saturated/oversaturated or undersaturated state (ignoring the possible transition state), as shown in the speed-flow fundamental diagram (Figure 3-3).
- The speed and flow rate over a time period, classified as having saturated traffic conditions, should evolve dynamically but consistently toward the same direction (i.e., either concurrently increasing or decreasing over the same time period).
- Over a time period where traffic conditions are at the undersaturated state (e.g., from 18:09:30 to 23:59:30, as shown in Figure 3-4), its flow rates and speeds will not trend in the same direction; i.e., moving in the opposite direction or no discernable trend.

With the above understandings, one can design the following test to assess if some speed-flow data in each time period over a target day will not exhibit the pattern deemed to be consistent with the expected quality.

- **Step 1:** Organize the archived detector data on a daily time-varying basis, as shown in Figure 3-4.
- **Step 2:** Divide the entire daily data into multiple time periods, based on either the significant change observed in its pattern or with the available method (e.g., change point detection with dynamic programming, Truong et al., 2020).
- **Step 3:** Perform the trend analysis with respect to the overall patterns of flow rate and speed data in each classified period (see Table 3-3) with the Mann-Kendall Test (Kendall, 1975) to identify its saturation state.
- **Step 4:** Divide the data in each classified period into small consecutive intervals of 15 minutes, and then perform the same trend analysis with respect to the speed and flow rate data in each short time interval.
- **Step 5:** Identify the consistency between the overall trend of the entire period with the estimated trend in each small interval to diagnose if any of such intervals contain data of unacceptable quality.

The results in Table 3-3 show the test results from the temporal trend test, where the overall traffic pattern during the 2nd period is identified as a saturated or oversaturated state. As such, the speed and flow rate data during this period cannot trend in opposite directions. With such information, one can then detect that some data in the 3rd and 22nd small intervals may not have the expected quality (see Table 3-4). One can perform the same steps of assessment of the data in all other divided time periods and compute the percentage of detector data not reaching the acceptable quality on this target day.

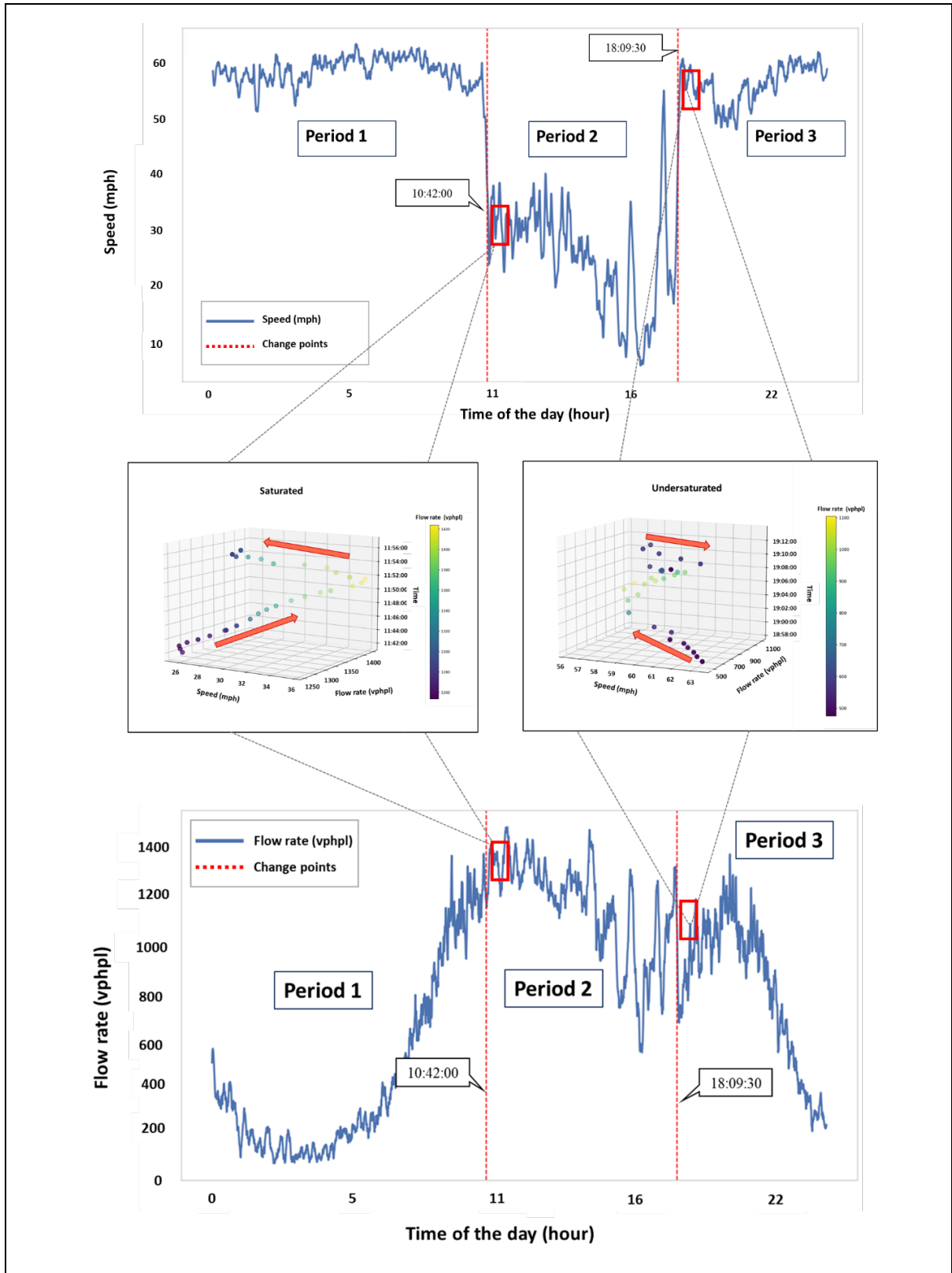


Figure 3-4: Temporal patterns for the Eastern Shore region's touring traffic detected by for sensor 317 (09/03/2018)

Table 3-3: Test of the saturation level during each time period

Mann-Kendall Test						
Period	1		2		3	
Time	00:00:00 to 10:42:00		10:42:00 to 18:09:30		18:09:30 to 23:59:30	
Number of recorded data	1284		895		700	
Trend	Speed	Flow Rate	Speed	Flow Rate	Speed	Flow Rate
	No Trend	Increasing	Decreasing	Decreasing	Increasing	Decreasing
H	False	True	True	True	True	True
P-value	0.069	0	0	0	$3.5 * 10^{-14}$	0
Traffic state	Undersaturated		Saturated		Undersaturated	

Table 3-4: Results of trend consistency test for small intervals in Period 2

Period 2								
Interval	1	2	3	4	5	6	7	8
Flow Speed	Increasing	Decreasing	Increasing	Decreasing	Increasing	Increasing	No Trend	Decreasing
	No Trend	No Trend	Decreasing	Decreasing	Increasing	No Trend	Increasing	Decreasing
Interval	9	10	11	12	13	14	15	16
Flow Speed	Decreasing	Decreasing	Decreasing	Stationary	Increasing	No Trend	No Trend	Increasing
	Decreasing	Decreasing	Decreasing	No Trend	Increasing	Decreasing	Increasing	Increasing
Interval	17	18	19	20	21	22	23	24
Flow Speed	Decreasing	Decreasing	Increasing	Increasing	Decreasing	Increasing	Increasing	Decreasing
	No Trend	Decreasing	Increasing	No Trend	Decreasing	Decreasing	No Trend	Decreasing
Interval	25	26	27	28	29			
Flow Speed	Decreasing	Decreasing	Decreasing	No Trend	Increasing			
	Decreasing	Decreasing	Decreasing	Decreasing	No Trend			

3.3 System Operation and Development

The flowchart in Figure 3-5 details the proposed two-stage screening process for detector quality assessment, where the target detector’s archived data over a prespecified period (e.g., one month) will progress to take Stage 2’s sequential tests if successfully passing through missing data and basic validity tests in the Stage 1 assessment.

Note that the three consecutive Stage 2 tests are designed to progressively raise the criteria to assess the data quality of the target detector. More specifically, the Stage 2A test is to be executed on the target detector’s archived speed-flow data, which have been filtered through the Stage 1 screening tests. Since the accuracy level of a traffic detector may vary with traffic conditions (such as congestion level), the Stage 2B test is proposed to further assess the data quality under three different traffic states: undersaturated, saturated, and transition/unstable states. Lastly, the Stage 2C test is designed to evaluate the target detector’s daily speed-flow temporal relations and to assess if their evolution patterns between saturated

and undersaturated periods actually trend toward the expected directions, as high-quality detector data should exhibit.

If more than 95% of the speed-flow data produced from the target traffic detector can pass the proposed two-stage sequential quality tests, then a field calibration is unnecessary, unless the data are expected to be used in high-precision, real-time adaptive traffic controls.

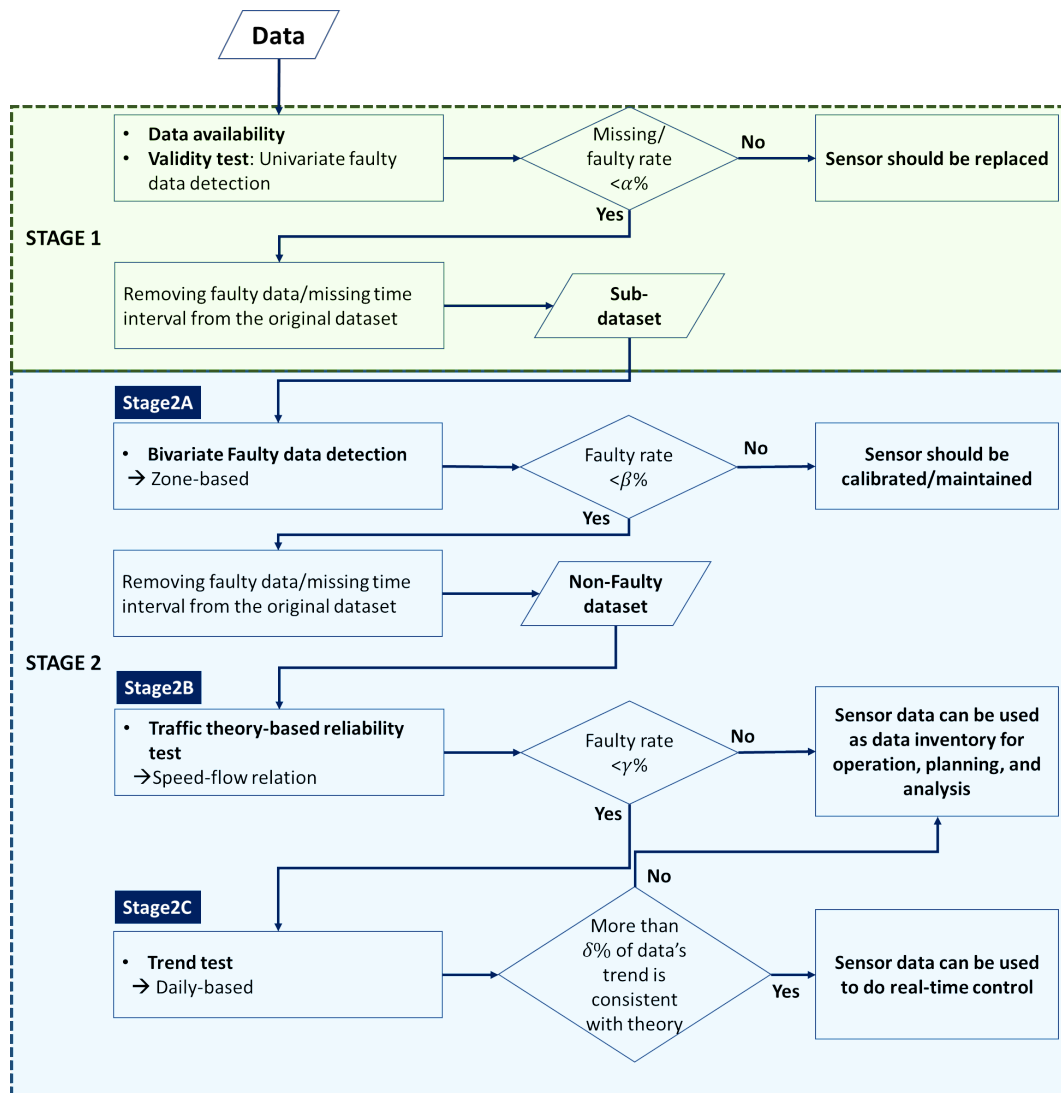


Figure 3-5: The operational flowchart for the entire system

The development process for the Stage 2A test

The procedures for developing the associated boundaries and control parameters of the Stage 2A test can be summarized as follows:

- **Step 1:** Select approximately one month or more data from a well-calibrated local detector and then apply the K-means clustering method to divide the dataset into the optimal distinct clusters (see Figure 3-2).
- **Step 2:** Identify the depth median (see Figure 3-6) by finding the point with the highest depth in each cluster (Tukey 1975).
- **Step 3:** Construct the inner-most polygon, named “bag” (see Figure 3-6), by finding the depth region (see Figure 3-6) containing half of the data points in each cluster (Rousseeuw, Ruts and Tukey, 1999).

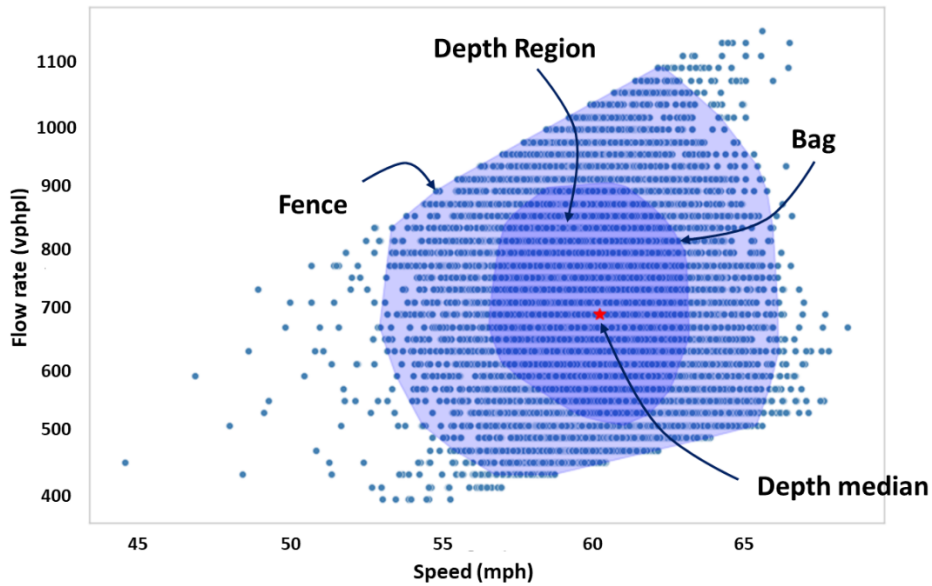


Figure 3-6: Illustrating the bagplot results from Zone 3 for constructing the boundaries

- **Step 4:** Determine the optimal inflating factor ε_i for zone i to obtain the range of its fence (see Figure 3-6) of a convex hull with the following objective function:

$$\text{Min} \quad z = \sum_{i=1}^4 \varepsilon_i \quad (3-1)$$

S. t.

$$\max(y_i^{k_i}) \geq \min(y_{i-1}^{k_{i-1}}), i = 3, 4; k_i = 1, 2, \dots, m_i \quad (3-2)$$

$$\max(x_1^{k_i}) \geq \min(x_2^{k_{i-1}}), k_i = 1, 2, \dots, m_i \quad (3-3)$$

$$N_i^{within} \geq 0.95 \cdot N_i^{total} \quad for \ i = 1,2,3,4 \quad (3-4)$$

Where ε_i denotes the inflating factor of zone i ; $x_i^{k_i}$ and $y_i^{k_i}$ denote the speed and flow rate of the k^{th} point on the convex hull of zone i , respectively; m_i denotes the total number of points on the convex hull of zone i ; N_i^{within} denotes the number of points within the fence of zone i ; and N_i^{total} denotes the total number of the points of zone i .

Note that Eq.1 should be subjected to the following constraints:

- the region of the fence, the outermost polygon defined in the previous study (Rousseeuw, Ruts, and Tukey, 1999), should cover more than 95% of the total data points (i.e., Eq.4); and
 - all constructed boundaries must be well connected without any gap area (i.e., Eq.2 and Eq.3).
- **Step 5:** Identify the corner points on the convex hull (see Figure 3-7) to formulate the boundaries for each zone, based on the following rules:
 - identify the points with the lowest speed and highest speed as the zone's vertices; and
 - find the two other points with the greatest slope and the most negative slope for each of the vertices.

A graphical illustration of the procedures for Zone 1 boundaries is shown in Figure 3-7.

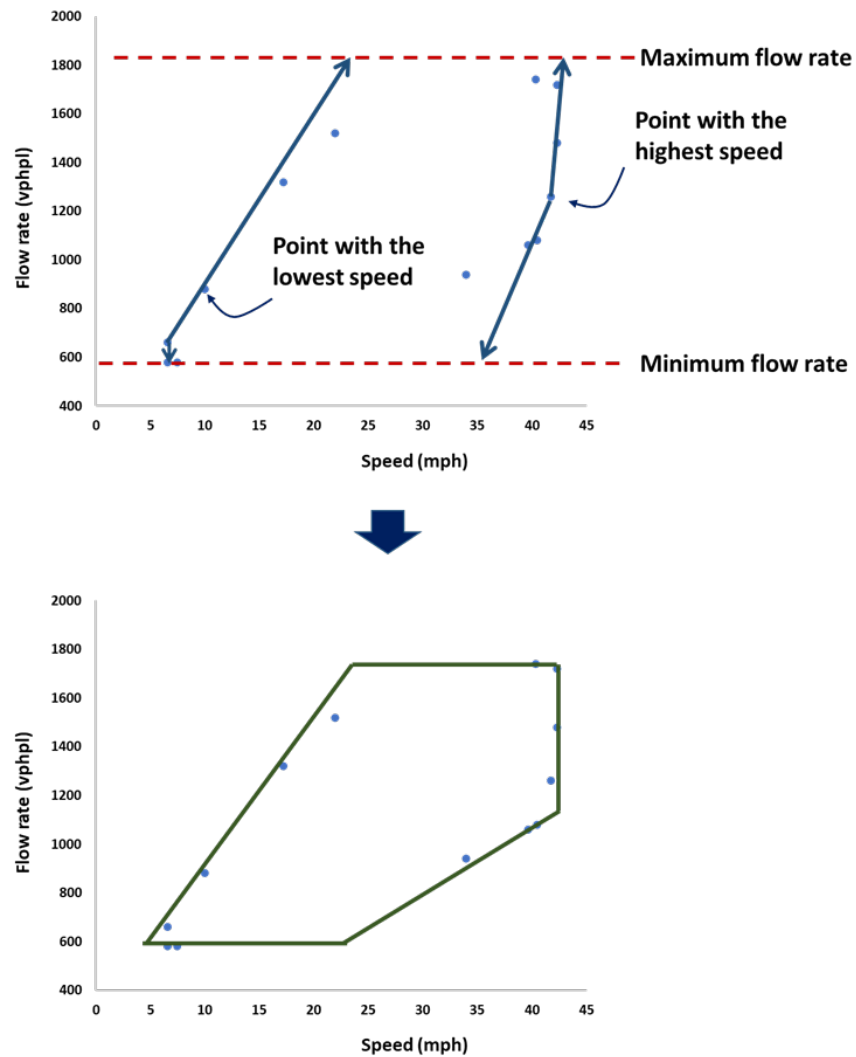


Figure 3-7: Boundaries identification for Zone 1

The development process for Stage 2B assessment test

Since the objective of the Stage 2B test is to identify the reasonable range of flow rate variation under a given speed at different traffic states, one can take the following steps to calibrate all essential equations for quality assessment:

- **Step 1:** Divide the speed-flow data passing the zone-based test into oversaturated, transition, and undersaturated clusters based on the minimum and maximum traffic speeds (e.g., 40 to 50 mph, see Figure 3-8) in the transition state estimated with the Gaussian Mixture Model (McLachlan, 1988).

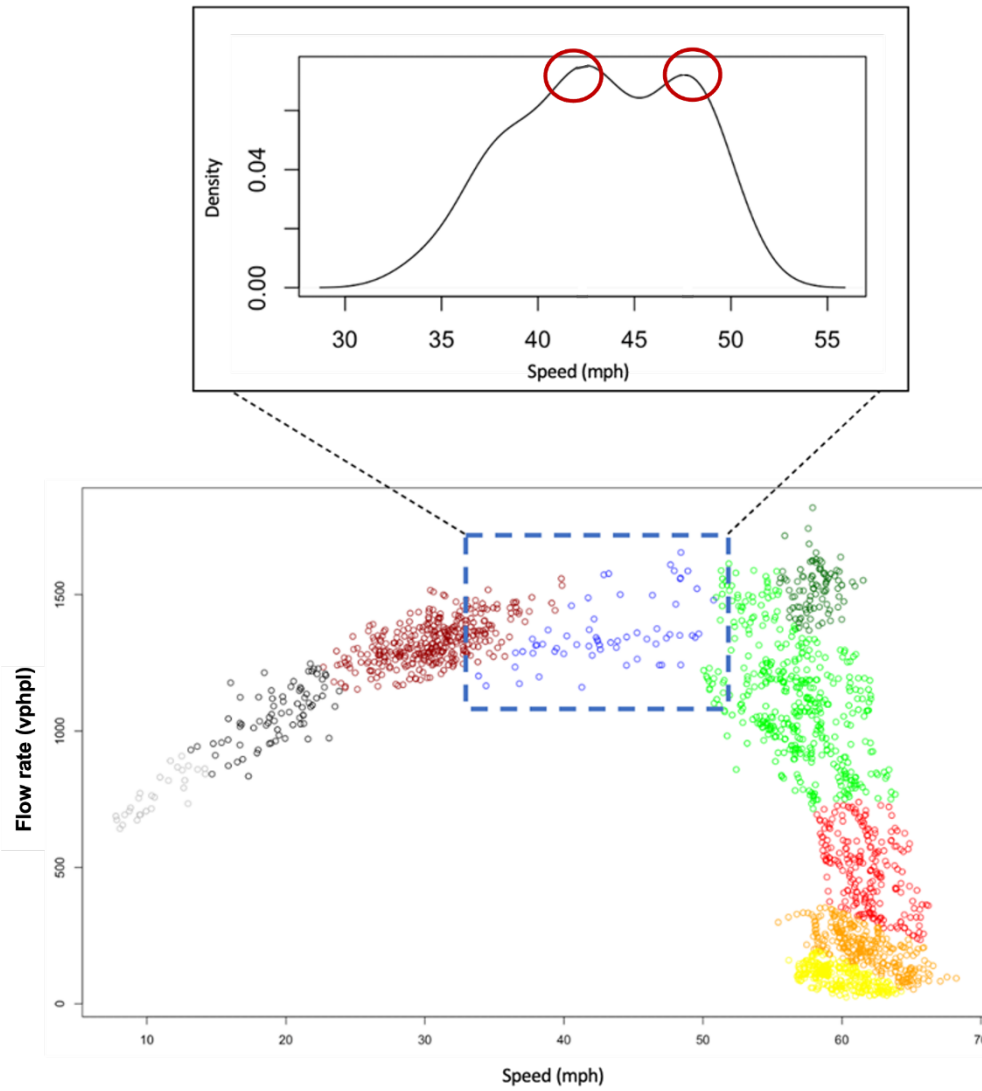


Figure 3-8: Identification of the transition zone

- **Step 2:** Fit all speed-flow data in the saturated cluster with the following function (Eq. 5) developed by Brilon and Lohoff (2011) by substituting k (density) with q/v ; perform the calibration with non-linear regression and apply the resulting 95% confidence interval as the quality control bounds (see Figure 3-9).

$$q = v \cdot b \cdot \ln \left(\left(\frac{2 \cdot v_0}{v} \right)^{\frac{1}{a}} - 1 \right) + c \quad (3-5)$$

where q and v denote the recorded flow rate and speed, respectively; v_0 denotes the free-flow speed; a , b , and c are the shape parameter, scale parameter, and transition parameter, respectively.

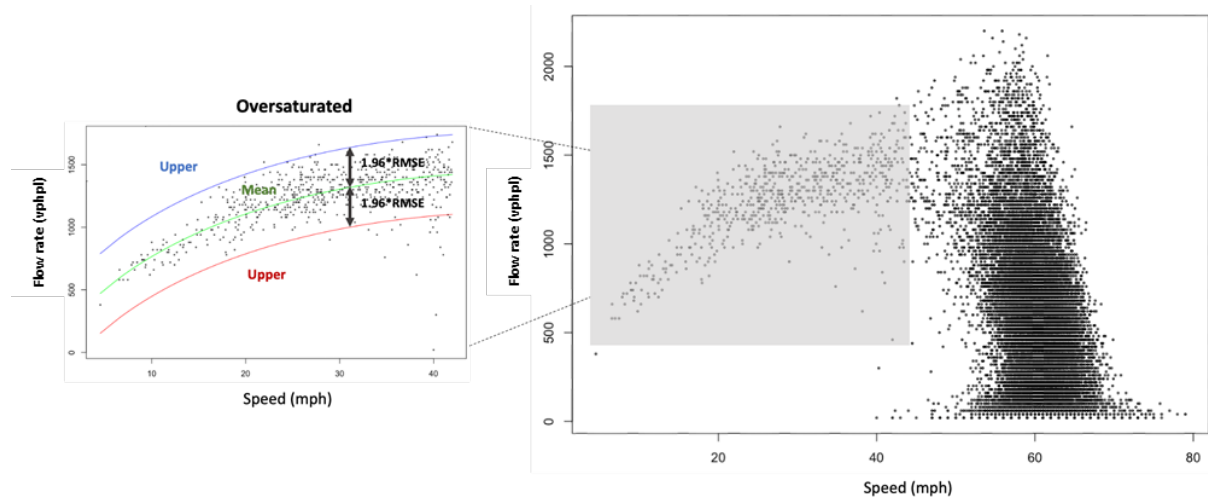


Figure 3-9: Development of speed-flow relationship for oversaturated traffic state (Mean Error: 2.12 vphpl)

- **Step 3:** Construct the zone-based control boundaries for the traffic conditions in the undersaturated state, but during peak hours (see Figure 3-10) with the following programming method to ensure that the control zone can cover the target percentage of data points (e.g., 95 %) with the minimum area:

$$\text{Min} \quad Z = A - n_{\text{within}} \quad (3-6)$$

S. t.

$$0 \leq x_1 \leq v_0 \quad (3-7)$$

$$0 \leq y_1 \leq C \quad (3-8)$$

$$A = \frac{1}{2}(x_1 + v_0 - 2 \cdot v_T^U)(C - y_1) \quad (3-9)$$

$$n_{\text{within}} \geq 0.95 \cdot n_{\text{total}} \quad (3-10)$$

Where A denotes the area of the trapezoid; n_{within} is the number of the points covered by the trapezoid, and n_{total} represents the total number of the points when it is undersaturated and during peak hours; x_1 and y_1 represent speed and flow rate, respectively; v_0 and C are the pre-specified free flow speed and capacity; and v_T^U is the maximum speed in the transition zone.

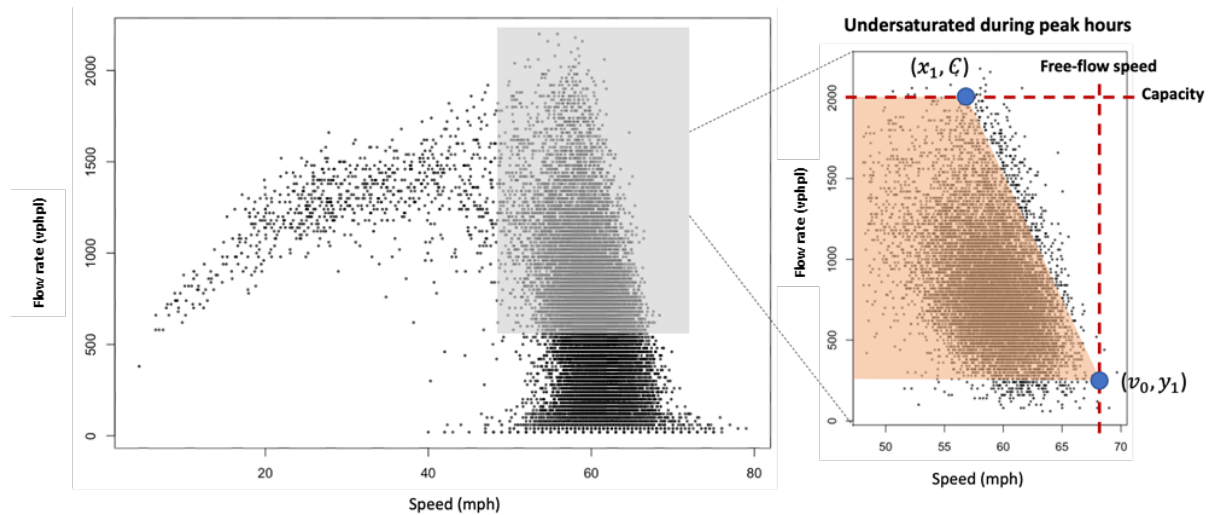


Figure 3-10: Development of speed-flow relationship for undersaturated traffic state during peak hours

- **Step 4:** Apply the traditional quality control method (e.g., three standard deviations) to set the acceptable range of variation for the traffic speed and flow rate data if they fall in the transition segment or if they are in the off-peak and undersaturated conditions because no discernable pattern differences can be identified for data distributed within these two traffic states.

3.4 System Application with the Customized Software

To facilitate the application, the research team has converted the above data-quality assessment process into a user-friendly computer software. One can then take the following simple steps to perform the assessment of a target detector's data quality:

- **Step 1:** Download the datafile from a selected traffic detector (see Figure 3-11).

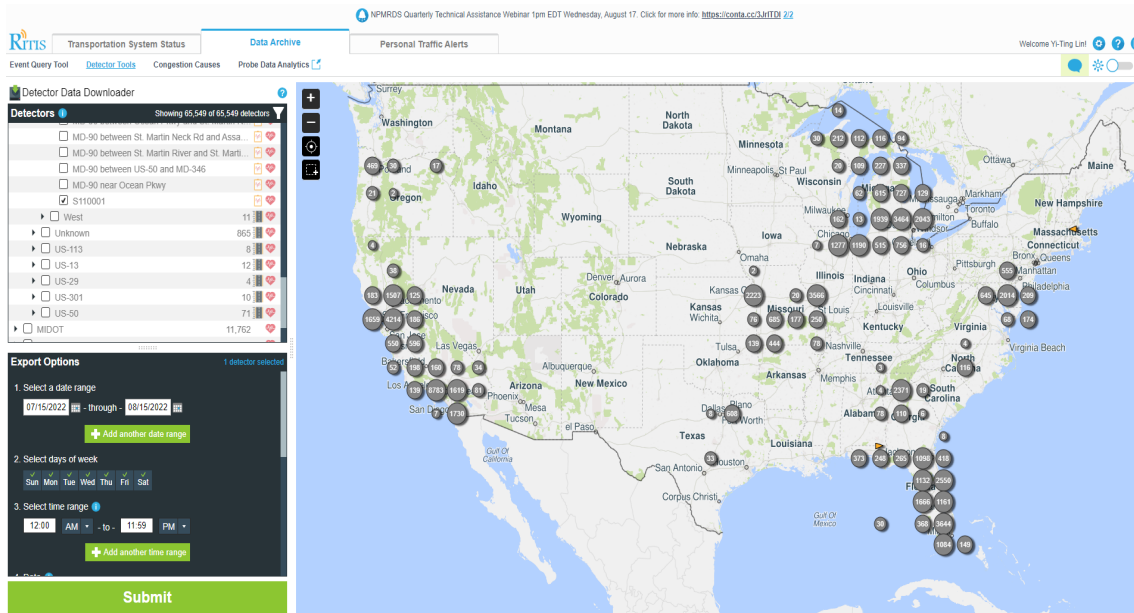


Figure 3-11: Log in to RITIS to download the sensor data of interest

- **Step 2:** Click the button “Start” to start the program.



Figure 3-12: Interface of the developed software for data quality assessment

- **Step 3:** Upload the sensor data downloaded from RITIS, and then press “**Save**” button and “**Next**” (Users can also specify the analysis period of interest at the optional section).

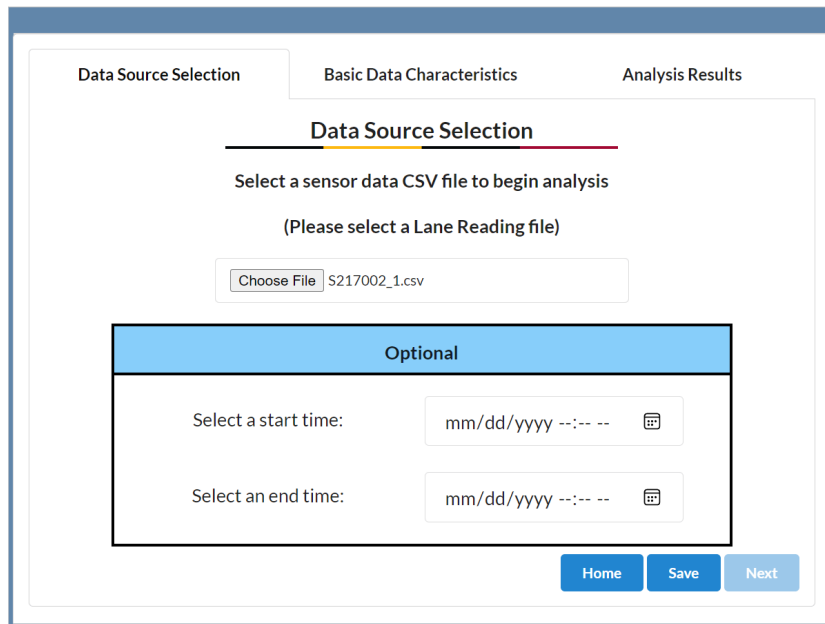


Figure 3-13: Interface page for uploading the target detector’s file

- **Step 4:** Press “**Next**” to see the analysis results, otherwise, press “**Back**” to revise the uploaded file.

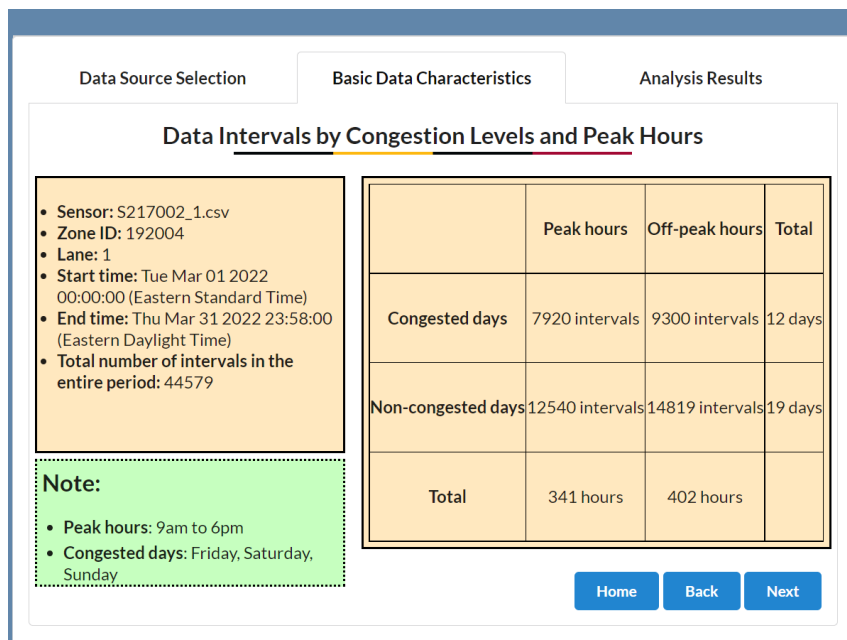


Figure 3-14: Interface page for summary of information associated with the uploaded file

- **Step 5:** Display the analysis results by (1) pressing the button of “**Download results**” to output detailed information regarding the faulty and missing data (step-6) or; (2) pressing “**Home**” to analyze the other sensor’s data (back to step-2); or (3) pressing “**Back**” to read the basic data characteristics (back to step-4).

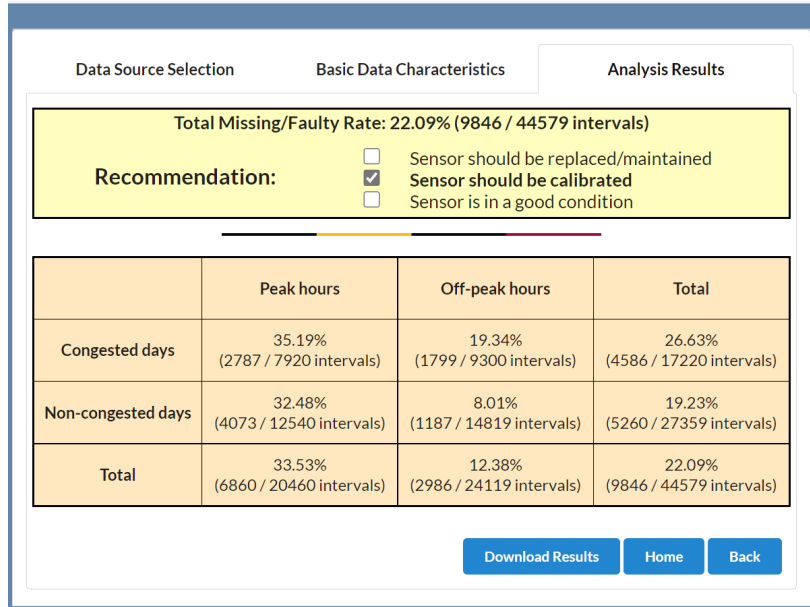


Figure 3-15: Interface page to show the assessment results

- **Step 6:** Select the details of interest by clicking on the different options, then press “**Download Results**”. An example of a downloaded file can be found in Appendix-A.

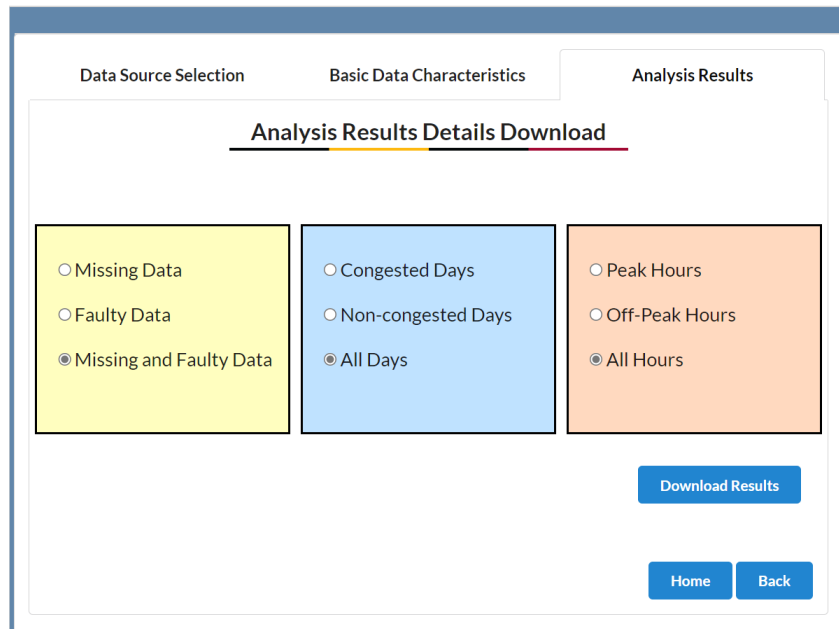


Figure 3-16: Interface page to download the analysis result details of interest

The assessment results for six candidate sensors with the above software are summarized in Table 3-4 and Table 3-5. Of those, only three (sensors 210, 323, and 301) have been well-calibrated; their speed-flow data quality has also been validated with field measurements. In contrast, the data from the time period during which sensor 11, sensor 13, and sensor 15 were not calibrated are also selected for assessing the effectiveness of the proposed quality evaluation algorithm. The screening results from State 1, Stage 2A, and Stage 2B are shown in the following tables.

Table 3-4: Evaluation results of well-calibrated sensors

Sensor ID		210	323	301
Location	Latitude	38.982	38.606	38.974
	Longitude	-76.162	-76.043	-76.265
Duration		Two months	27 Days	One month
Number of recorded data		170523	74604	83652
Quality Screening Results				
Stage 1		4.5% (8038/178560)	4.1% (3156/77760)	3.2% (2777/86400)
Stage 2A		3.8% (6394/170522)	0.6% (445/74604)	2.3% (1946/83623)
Stage 2B		1.2% (2131/170522)	0.4% (300/74604)	3.2% (2699/83623)
Total faulty rate		5.0% (8526/170523)	1.0% (745/74604)	5.6% (4674/83652)

Table 3-5: Screening results of low-quality sensors

Sensor ID		11	13	15
Location	Latitude	38.372	38.059	38.295
	Longitude	-75.260	-75.545	-75.639
Duration		Two months	Two months	Two months
Number of recorded data		173591	176902	177659
Quality Screening Results				
Stage 1		2.8% (4973/178560)	0.9% (1659/178560)	0.5% (905/178560)
Stage 2A		21.2% (36865/173587)	46.3% (81914/176901)	16.0% (28472/177655)
Stage 2B		6.7% (11592/173587)	0.6% (1091/176901)	0.4% (756/177655)
Total faulty rate		27.9% (48461/173591)	46.9% (83006/176902)	16.5% (29232/177659)

Figure 3-17 shows the speed-flow relationship of the three well-calibrated sensors during the selected time period for evaluation, where sensor 210 and sensor 301 contain some traffic states in the saturated or oversaturated states. For comparison, the speed-flow relationships from those sensors, which have not been calibrated, are also displayed in Figure 3-18. Noticeably, the spatial distributions of such speed-flow data points are dispersed quite far away from the theoretical speed-flow relationship, an indication of less reliable quality.

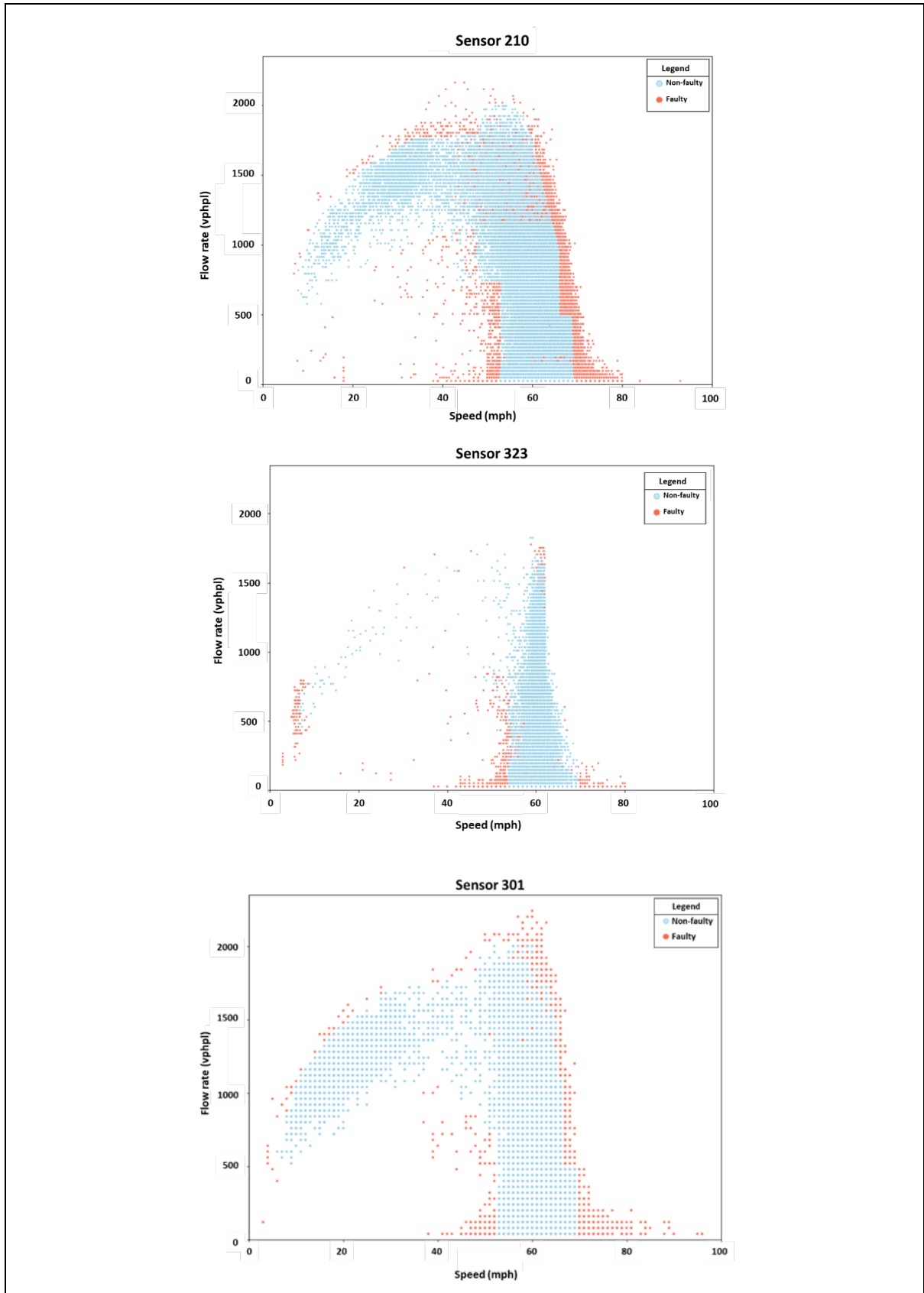


Figure 3-17: Graphical illustration of the speed-flow relationships from three well-calibrated sensors

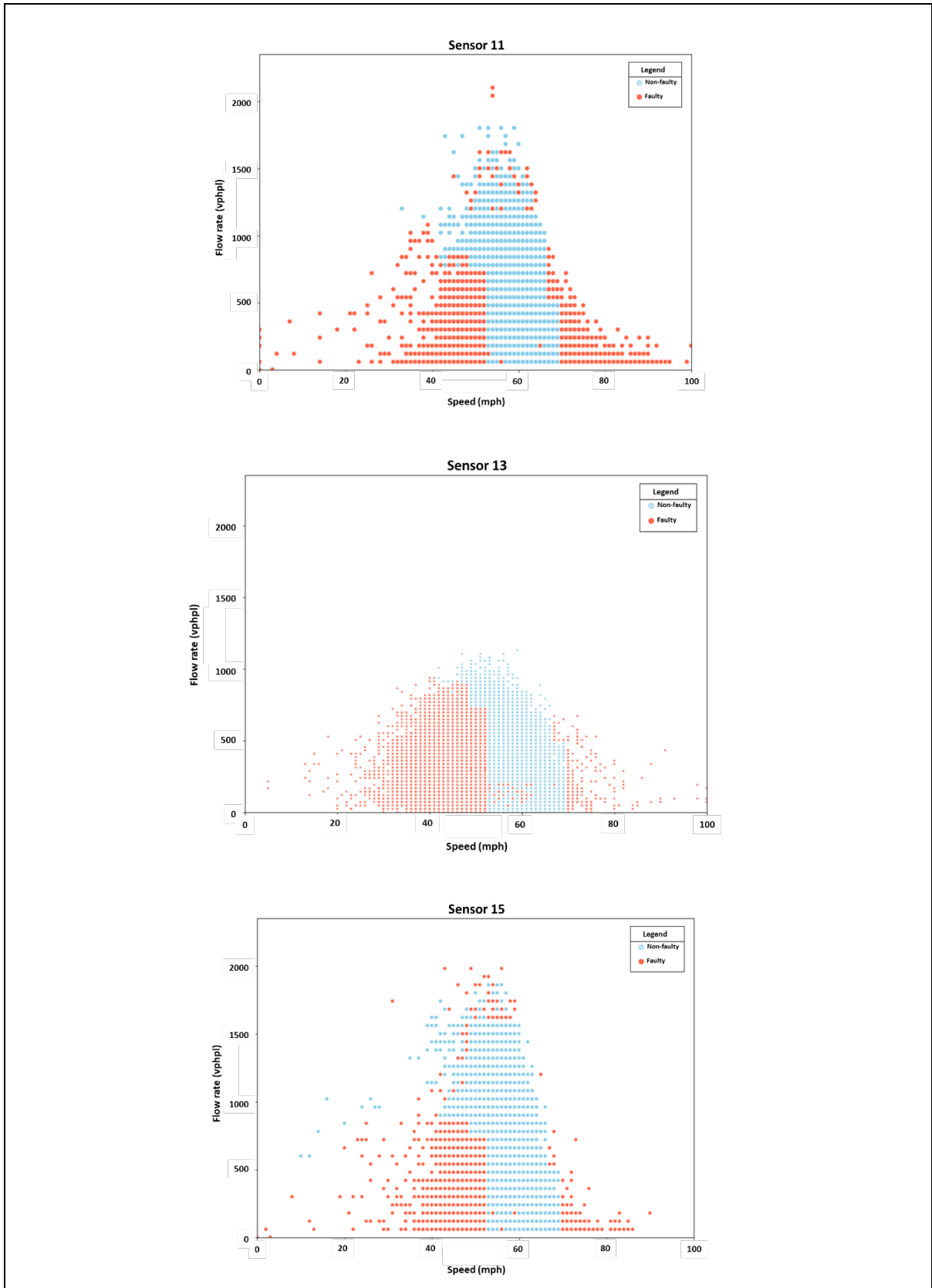


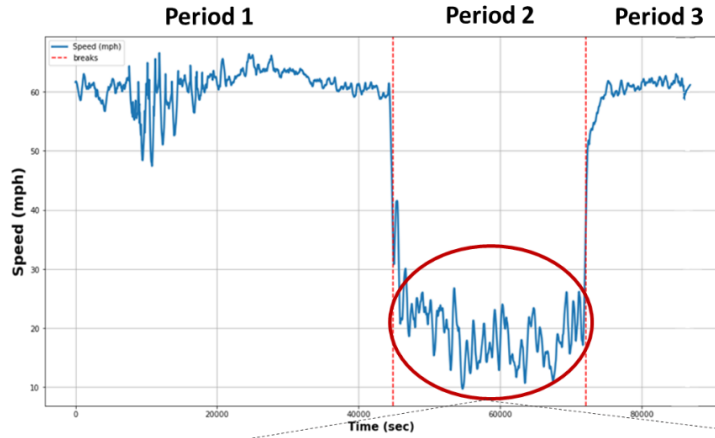
Figure 3-18: Graphical illustration of the speed-flow relationships from three not-calibrated sensors

Stage 2C test results

Note that this test shall be conducted only if the selected detector dataset contains some saturated or oversaturated traffic states, as shown in the data from sensor 210 and sensor 301. Table 3-6 summarizes the result of Stage 2C tests with respect to sensor 210 and sensor 301, revealing that more than 90% of the speed and flow data from both sensors on the selected day exhibit consistent temporal patterns over different time periods. Figure 3-19 further shows all statistics associated with the trend consistency tests that contribute to the final results in Table 3-6.

Table 3-6: Examples of Stage 2C test results

Sensor ID	210			301		
Date	7/16/2017			09/03/2018		
Number of recorded data	2736			2880		
Time	Period 1	Period 2	Period 3	Period 1	Period 2	Period 3
	00:00:00 to 07:31:30	07:31:30 to 15:58:00	15:58:00 to 23:59:30	00:00:00 to 12:27:00	12:27:00 to 20:02:00	20:02:00 to 23:59:30
Traffic state	Undersaturated	Saturated	Undersaturated	Undersaturated	Saturated	Undersaturated
Number of time intervals	28	33	29	49	30	15
Number of time intervals consistent with traffic state of the period	28	29	28	49	30	15
Consistence rate	100%	88%	100%	100%	100%	100%
Total consistence rate	94.4% (85/90)			100% (94/94)		



	Time interval	1	2	3	4	5	6	7	8	9	10	11	12	13	14	15
Period 2	Flow rate	no trend	increasing	no trend	no trend	no trend	no trend	no trend	no trend	no trend	increasing	decreasing	increasing	increasing	no trend	decreasing
	Speed	no trend	increasing	decreasing	no trend	no trend	no trend	no trend	no trend	no trend	no trend	increasing	decreasing	increasing	increasing	no trend
	Time interval	16	17	18	19	20	21	22	23	24	25	26	27	28	29	30
	Flow rate	no trend	decreasing	no trend	increasing	no trend	decreasing	no trend	no trend	decreasing	decreasing	increasing	no trend	no trend	decreasing	no trend
	Speed	no trend	decreasing	no trend	no trend	no trend	decreasing	no trend	decreasing	decreasing	decreasing	increasing	no trend	decreasing	no trend	decreasing

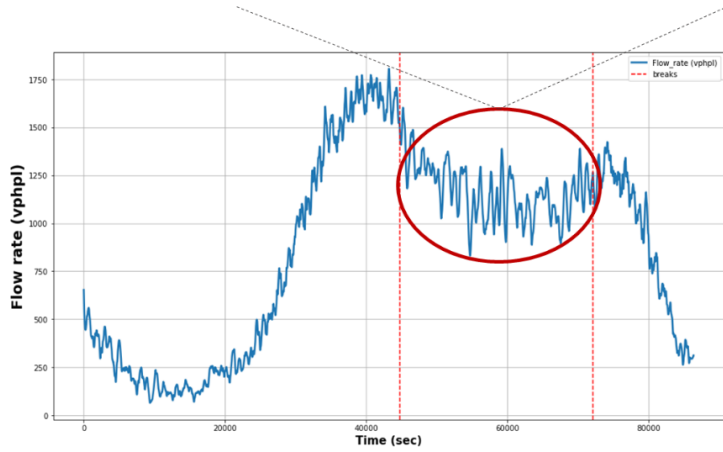


Figure 3-19: An example of Stage 2C test based on sensor 301 (09/03/2018)

Chapter 4: Selection of Locations for Eastern Shore Sensor

Deployment

4.1 Introduction

This chapter presents the method for identifying the list of potential detector locations for the Eastern Shore's traffic surveillance system, based on the expected effectiveness from the perspectives of traffic monitoring and congestion control. For convenience of applying the proposed method to other regions, the presentation will first provide a step-by-step description of the proposed method, including the embedded criteria and expected output from each primary stage in the identifying and selection process. This is followed by a detailed case study with traffic patterns for the entire Eastern Shore region, focusing on the analysis results from the following principal steps of the proposed method:

- define the purposes of the target sensor deployment;
- analyze congestion patterns over the target roadway network and decompose them into clusters of congested segments based on the available time-varying speed information from probing vehicle reports or traffic information from Google;
- investigate the spatial and temporal distributions of congestion patterns over each identified congested highway segment;
- identify the set of ideal sensor locations based on the purposes of deployment;
- identify the locations of existing infrastructure available for sensor deployment; and
- finalize the list of recommended locations for sensor deployment.

Concluding comments regarding the application results, along with some critical sensor deployment issues, will be highlighted in the last section.

4.2 Method for Selecting Detector Deployment Locations

The entire implementing process for the proposed method can be divided into the following steps:

Step 1: Finalize the main purpose for the deployed sensors.

Most deployed sensors are expected to perform some or all of the following functions:

- traffic monitoring only, such as the average speed, flow rate, and traffic patterns on an

hourly basis;

- design of traffic control strategies with real-time traffic flow characteristics, including speed, flow rate, and occupancy (if available) over each the per-specified time, e.g., per minute or per five minutes; and
- advance travel information systems, such as offering real-time travel time prediction during both recurrent and non-recurrent congestion, or detouring route guidance.

Note that the detection zone by deployed sensors must cover all traffic streams moving over the target congested roadway segment if the primary purpose is to provide the first function only. Otherwise, the deployed sensors must provide the spatial coverage of an entire roadway's tempo-spatial traffic patterns, including their congestion formation and dissipation over time and potential bottleneck areas.

Step 2: Analyze and decompose the congestion patterns over the roadway network.

This step is to analyze the congestion pattern over the target highway and decompose its spatial distribution into several clusters so that one can identify the priority of locations for detector deployment on highway segments in the target roadway network. Such a task of decomposition and priority ranking is especially essential if the available budget for detector deployment is a major constraint.

Figure 4-1 shows the spatial distribution of all congested segments over the Eastern Shore region and their respective boundaries to be covered by traffic detectors. Figure 4-2 presents the information of time-varying speed distribution to identify the locations and spatial coverages of those congested segments, where the roadway network from Ocean City to Bay Bridge is decomposed into seven congested roadway segments.

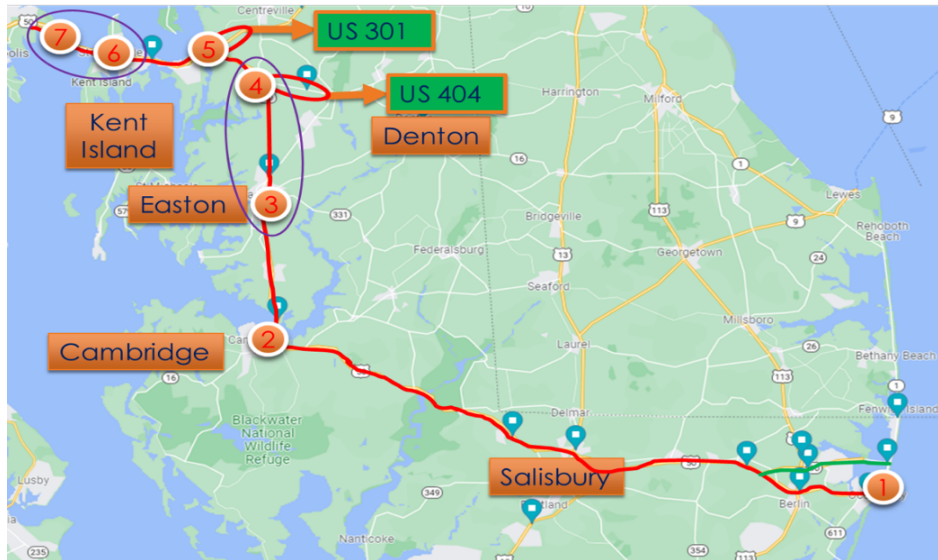


Figure 4-1: Graphical illustration of the decomposed congestion patterns within the Eastern Shore region

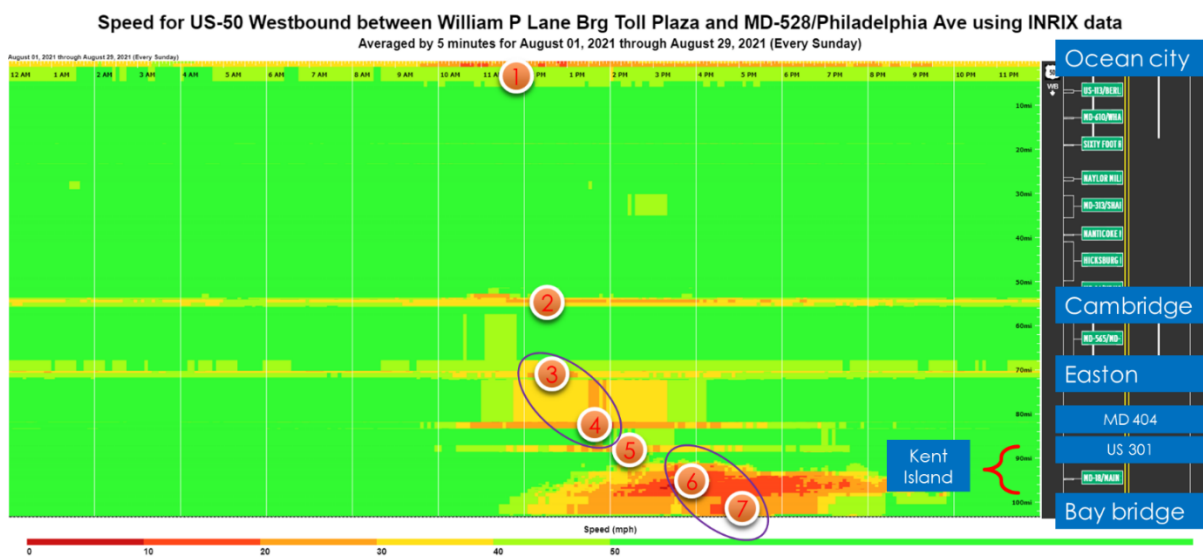


Figure 4-2: Example of the speed-evolution data for identifying and decomposing congestion patterns

Step 3: Investigate the spatial and temporal distributions of congestion patterns over each identified congested highway segment.

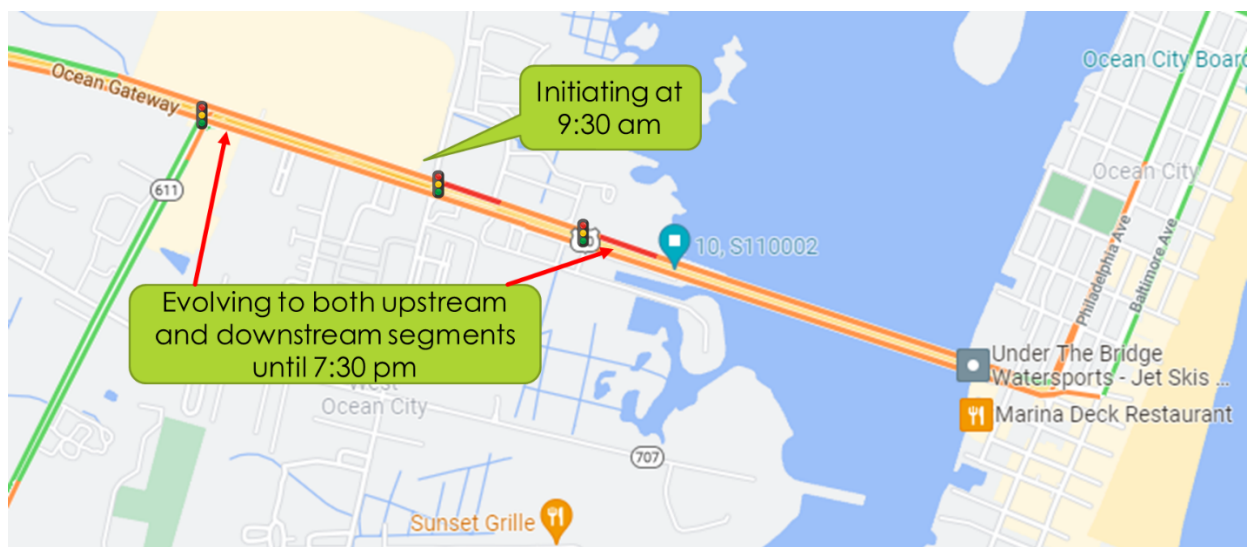
As shown in Figure 4-3, the analyses to be done at this step are identification of the starting and ending times of the congestion pattern over the target congested segment and its precise spatial distribution, including the maximum queue distance or spillover location. Traffic streams from either side streets or major traffic generation centers (e.g., a shopping mall) should also be identified. With such information, one can then finalize the preliminary

set of optimal detector locations for monitoring traffic conditions (e.g., speed and volume) on the main roadway, and then select additional detector locations based on the proposed control strategies to further characterize the traffic impacts due to the detected congestion pattern.

Figure 4-3 shows the analysis results of congestion patterns for the Cluster 1 congested segment, including both the spatial and temporal evolutions of traffic queues over the main arterial and side streets.

Sensor Deployment at the Congestion Segments

Congestion location 1: OC drawbridge



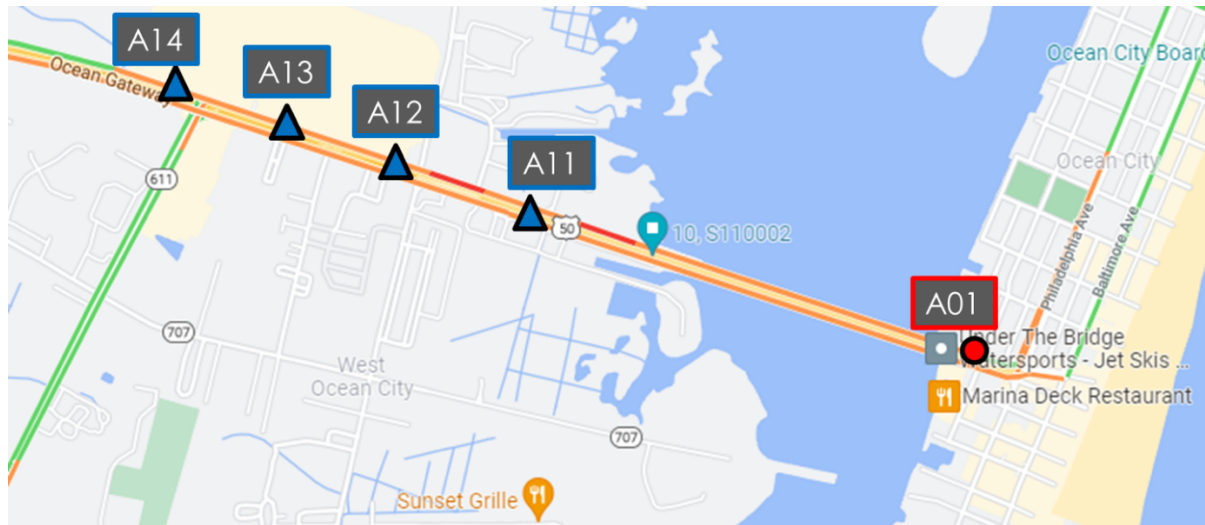
Congestion pattern
9 am - 8 pm, Short section, Side street also congested during peak hours
Causes congestions on OC

Figure 4-3: Results of congestion pattern analysis for Cluster 1 congested highway segment within the Eastern Shore region

Step 4: Identify the set of ideal sensor locations based on the purposes of such a deployment.

The focus of this step is to identify the optimal set of detector locations for each target application without considering the budget constraints. For example, Location A01 (see Figure 4-14) is selected as the detector location mainly for monitoring traffic volume and flow speed moving onto US 50. In contrast, detector locations from A11-A14 are proposed to capture the spatial distribution of the congestion pattern, including the onset point of the traffic queues and some congestion-contributing factors, such as intersection turning volumes (see A11 in Figure 4-14). The real-time speeds, flow rates and turning ratios from such detectors will provide essential information for the design of dynamic traffic control strategies such as reversed signal progression or variable speed control.

Ideal locations for traffic monitoring and traffic controls



- Traffic flow monitoring
- ▲ Identifying congestion patterns and spillovers



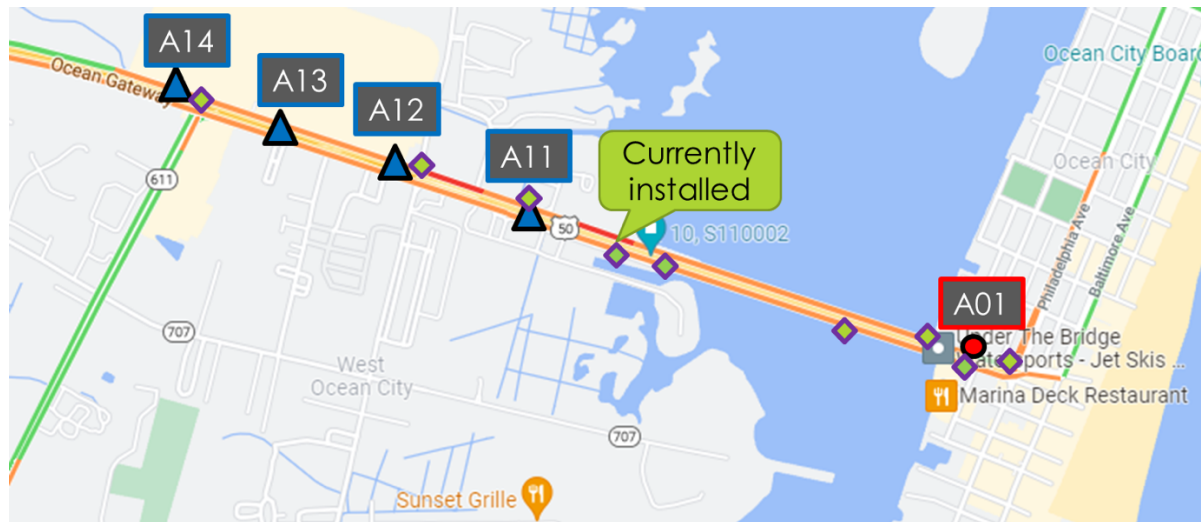
Figure 4-4: Detector locations selected for different application needs

Step 5: Identify locations of existing infrastructure available for sensor deployment and finalize the deployment plan.

To minimize the deployment cost, one shall first consider mounting proposed sensors on existing infrastructure or traffic control devices (such as signal head, utility pole) as long as their resulting spatial coverage of traffic conditions does not differ significantly from that provided by the detectors deployed at nearby optimal locations. Figure 4-5 presents the execution results from this step, displaying the precise GPS coordinates for each proposed detector and the nearby available traffic infrastructure for deployment. For example, the proposed detectors, A11, A12, and A14 for congestion control can all be mounted on the

intersection’s signal posts. However, a new roadside post would be needed for mounting detector A13 if detecting the target intersection’s approaching volume and turning ratios are viewed as essential.

Recommended sensor locations



- Traffic flow monitoring
- ▲ Identifying congestion patterns and spillovers
- ◆ Existing infrastructure

NO.	GPS-COORDINATE	LOCATION TYPE	NEARBY POLES?	PRIORITY
A01	38.331733, -75.087969	Roadside	Yes	Required
A11	38.336303, -75.105415	Intersection	Yes	Desired
A12	38.337997, -75.111963	Intersection	Yes	Desired
A13	38.337242, -75.109105	Roadside	No	Optional
A14	38.338032, -75.112103	Intersection	Yes	Desired

Figure 4-5: The list of recommended locations and available infrastructure for detector deployment for Cluster 1 congested highway segment in the Eastern Shore region

4.3 List of Locations Recommended for Detector Deployments in the Eastern Shore Region

With the same five-step process illustrated above, this section summarizes the application results for all remaining congested highway segments in the Eastern Shore region, as follows:

Cluster 2 congested highway segment

Figure 4-6 illustrates the results of congestion pattern analysis for the Cluster 2 congested highway segment within the Eastern Shore region. Figure 4-7 summarizes the list of locations for detector deployment based on the detected congestion patterns. The list of detector locations that are closed to existing traffic infrastructure are also presented in this figure.

Notably, detector B01 is essential for traffic monitoring need, offering traffic speed and volume entering this segment for responsible traffic engineers to prepare any necessary actions in advance, and for timely update of the travel information system. The set of detectors, B12, B13, and B14, is proposed for capturing the formation and dissipation of the segment's congestion pattern from peak to off-peak periods. Such data are critical for design of traffic control strategies to prevent the traffic queue spillback and mitigate the congestion level.

If the budget for sensor deployment is not of concern and minimizing traffic congestion is the foremost objective, then one can also address the impacts of vehicles from the side-streets on the primary roadway segment's queue formation and speed disturbance. Hence, deployment of detectors B02-B04 are suggested for such a need.

Congestion location 2: Cambridge



Congestion pattern

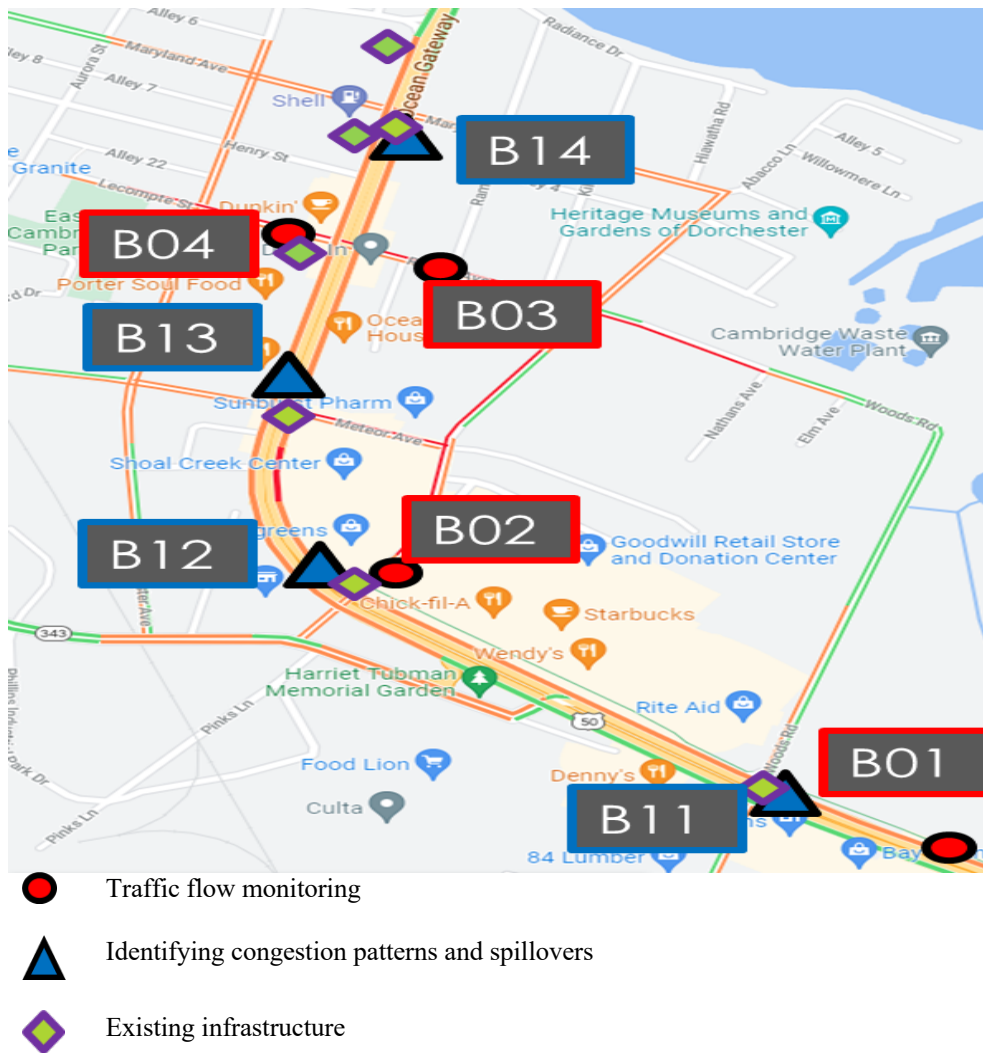
10 am - 4 pm

Impacts by local traffic

Multiple signalized intersections involved

Figure 4-6: Results of congestion pattern analysis for Cluster 2 congested highway segment in the Eastern-shore region

Recommended sensor locations



NO.	LOCATION	LOCATION TYPE	NEARBY POLES?	PRIORITY
B01	38.557308, -76.058088	Roadside	No	Required
B02	38.561650, -76.064510	Roadside	No	Optional
B03	38.566189, -76.064372	Roadside	No	Optional
B04	38.566589, -76.065812	Roadside	No	Optional
B11	38.558480, -76.060475	Intersection	Yes	Optional
B12	38.561434, -76.065326	Intersection	Yes	Desired
B13	38.564209, -76.065595	Intersection	Yes	Desired
B14	38.567898, -76.064449	Intersection	Yes	Desired

Figure 4-7: The list of recommended locations and available infrastructure for detector deployment for Cluster 2 congested highway segment in the Eastern Shore region

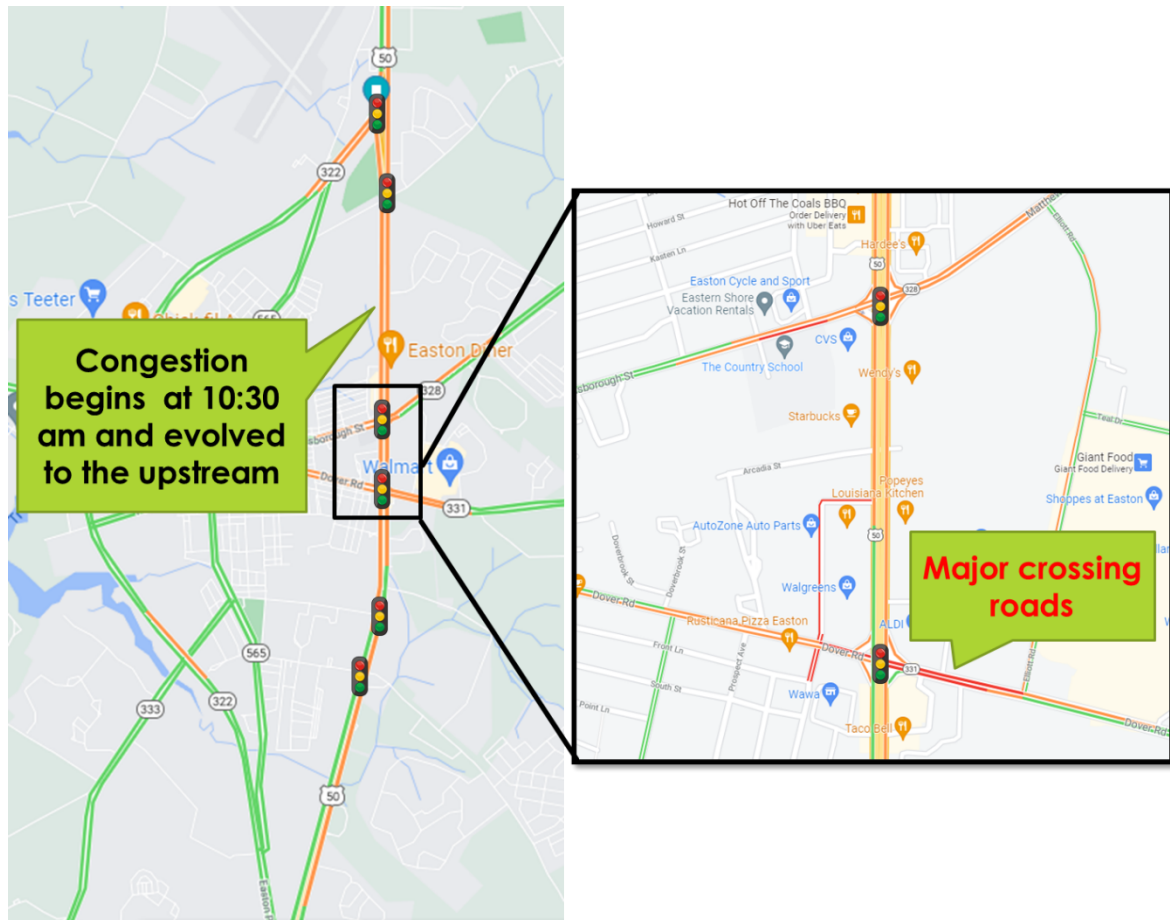
Cluster 3 congested highway segment

Figure 4-8 illustrates the results of congestion pattern analysis for the Cluster 3 congested highway segment within the Eastern Shore region, where cross-traffic flows intersect with heavy traffic at US 50's two major intersections are the main contributors for congestion formation over this highway segment. The list of locations for deploying traffic detectors, based on such congestion patterns, is shown in Figure 4-9, including the existing traffic infrastructure that is available for mounting the detecting devices.

Notably, there are six candidate locations (i.e., C01, C11, C12, C13, C14, C15) for detector placement close to existing traffic or utility poles, where C01 is essential for traffic monitoring and the remaining five sensor locations are for tracking the temp-spatial congestion pattern. Such data are critical for design of traffic control strategies to prevent the traffic queue spillback and mitigate congestion. For example, as shown in Figure 4-10, C15 is proposed to capture both the intersection's volume distribution and highway merging flows; C12 and C13 are mainly for monitoring turning traffic volumes at intersections.

Because intersections on US 50 in this area possess a high turning volume and contribute significantly to the main roadway's formation of oversaturated traffic conditions, one may consider deploying some additional detectors to measure the time-varying traffic flows from major crossing roads if the budget for sensor deployment is sufficient. Note that real-time turning traffic information is essential for design of control strategies to minimize the likelihood of turning queue spillback. Deployment of detectors C02-C0 and C11 are suggested for such a need.

Congestion location 3: Easton



Congestion pattern:
1 pm - 2 pm
Long section
May evolve from downstream (No. 4)
Impacts local traffic
Multiple oversaturated signalized intersections

Figure 4-8: Results of congestion pattern analysis for Cluster 3 congested highway segment in the Eastern Shore region

Recommended sensor locations



- Traffic flow monitoring
- ▲ Identifying congestion patterns and spillovers
- ◆ Existing infrastructure

NO.	LOCATION	LOCATION TYPE	NEARBY POLES?	PRIORITY
C01	38.748521, -76.065804	Roadside	Yes	Required
C02	38.772194, -76.059027	Roadside	No	Optional
C03	38.772707, -76.061791	Roadside	No	Optional
C04	38.777918, -76.058795	Roadside	No	Optional
C05	38.776870, -76.062335	Roadside	No	Optional
C11	38.759947, -76.061858	Intersection	Yes	Optional
C12	38.772829, -76.060169	Intersection	Yes	Desired
C13	38.777960, -76.060142	Intersection	Yes	Desired
C14	38.793655, -76.060055	Intersection	Yes	Optional
C15	38.802859, -76.059997	Intersection	Yes	Desired

Figure 4-9: List of results of congestion pattern analysis for Cluster 3 congested highway segment in the Eastern Shore region

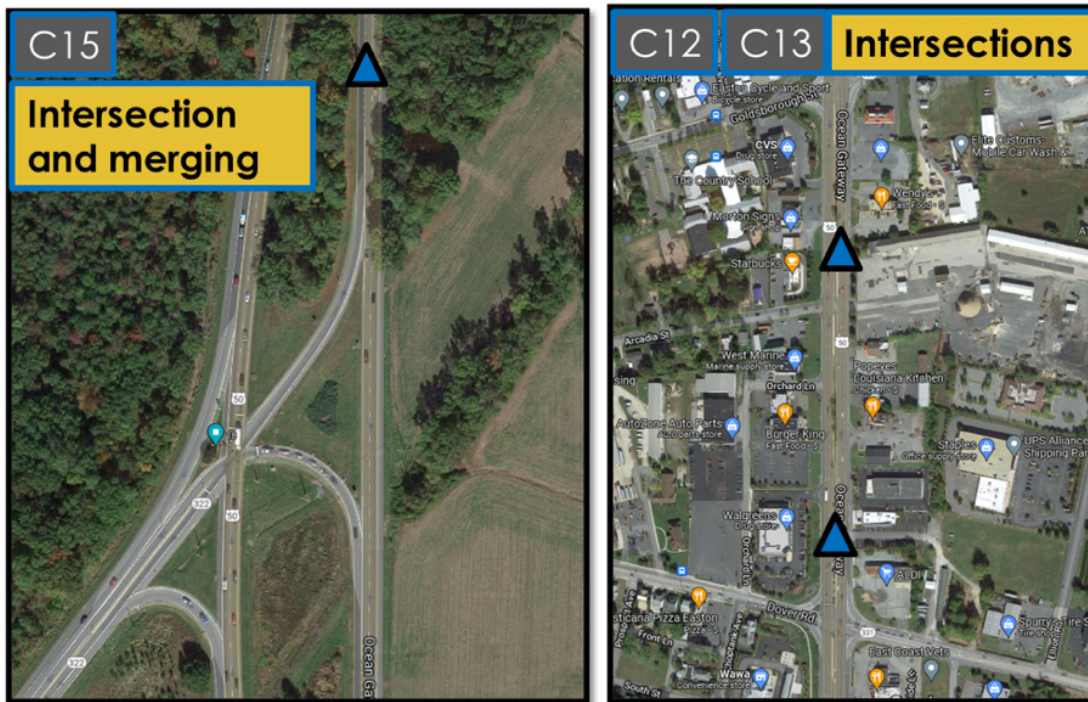


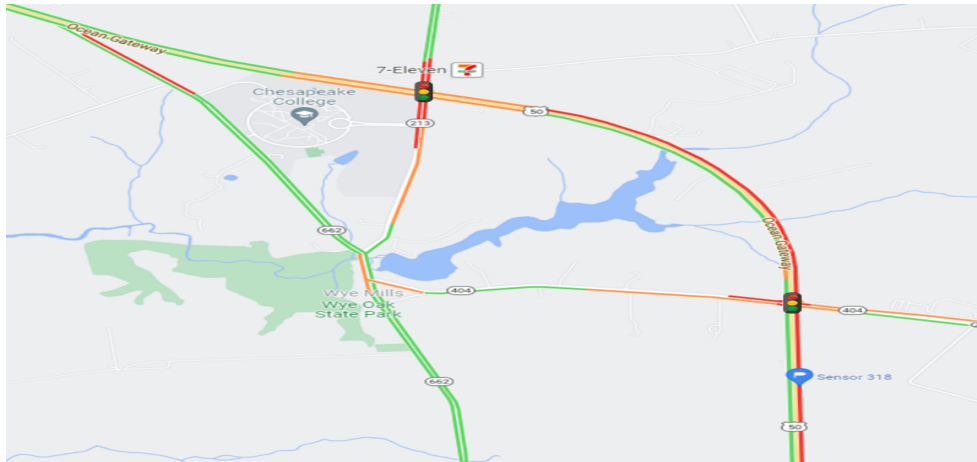
Figure 4-10: Examples of detector deployment for monitoring turning traffic volumes at major intersections

Cluster 4 congested highway segment

The Cluster 4 congestion pattern over this segment of US 50, as shown in Figure 4-11, mostly begins at 10am and dissipates around 4pm, typically propagating queues back. Two major intersections, US 50 & MD 404 and US 50 & MD 213, are the main contributors to the resulting congestion on US 50, which often reach the saturation level and spill traffic queues back to the upstream segment.

The analysis results, as shown in Figure 4-13, indicate the need to deploy at least one detector at D01 to monitor traffic volumes and speeds over this segment. However, it would need additional five detectors placed at the identified roadside locations (i.e., D02-D05 and D12) and at intersection D11 to fully capture the time-varying evolution of congestion patterns. The information can also be used to design either reversed arterial signal progression strategies or dynamic speed control plan for congestion mitigation. Figure 4-12 further shows the geometric features of the two intersections, which are the bottlenecks for this area. The precise locations for detectors to monitor the flow patterns at these two congested intersections are also shown in Figure 4-13.

Congested intersections between US 50 and MD 404 & MD 213



Congestion pattern
10 am - 4 pm
Long congested segment
Evolves to Easton
Two major signalized intersections
Two major crossing streets

Figure 4-11: Results of congestion pattern analysis for Cluster 4 congested highway segment in the Eastern Shore region

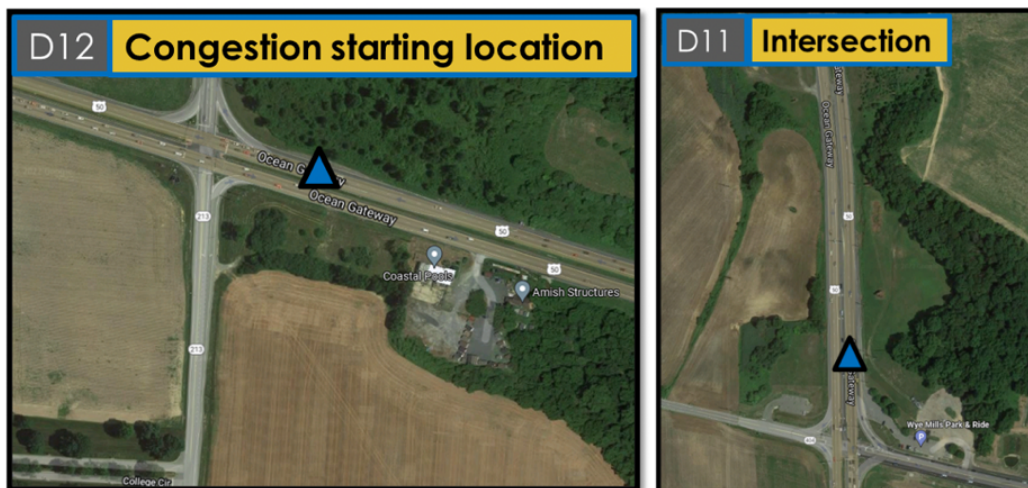


Figure 4-12: Geometric features of the two congested intersections and suggested locations for detector deployment

Recommended sensor locations



NO.	LOCATION	LOCATION TYPE	NEARBY POLES?	PRIORITY
D01	38.929471, -76.062214	Roadside	No	Required
D02	38.938950, -76.060247	Roadside	No	Desired
D03	38.939660, -76.064484	Roadside	No	Desired
D04	38.955490, -76.078468	Roadside	No	Desired
D05	38.952853, -76.078564	Roadside	No	Desired
D11	38.941726, -76.062521	Intersection	Yes	Desired
D12	38.954178, -76.077355	Roadside	Yes	Desired

Figure 4-13: List of detectors recommended for Cluster 4 congested highway segment in the Eastern Shore region

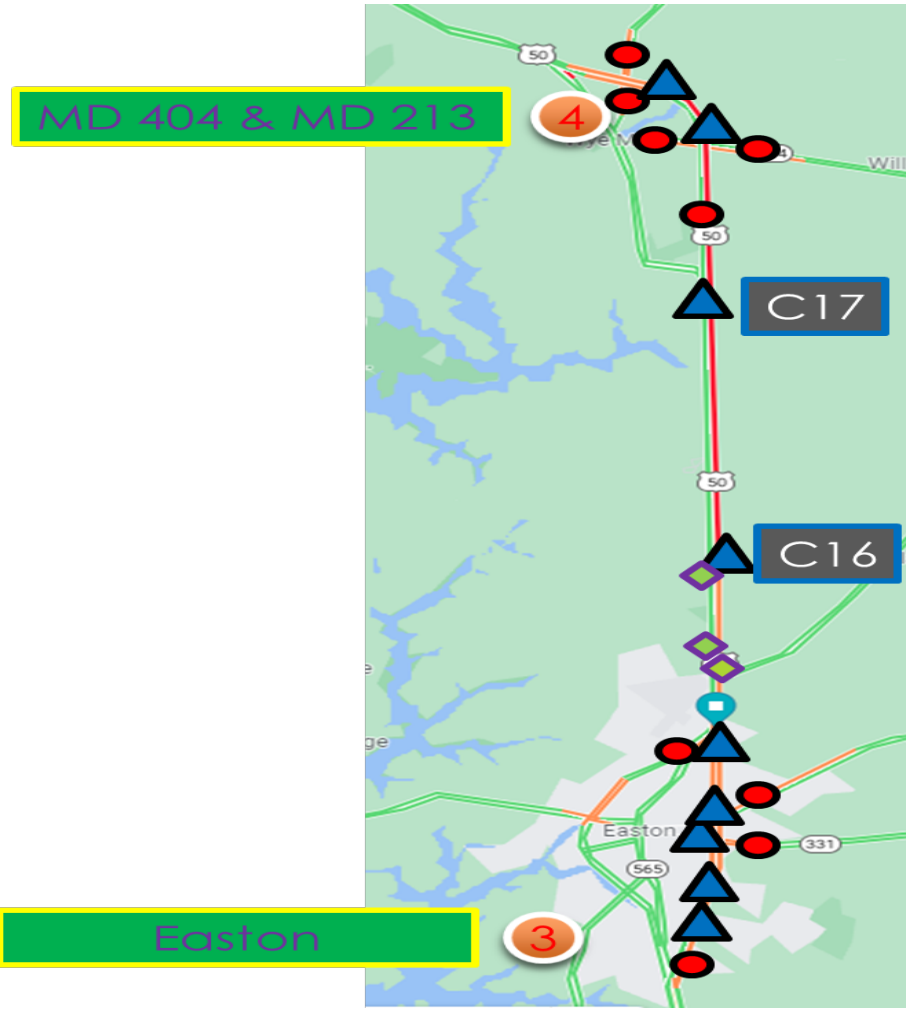
Cluster 5 congested highway segment: between congestion segments 3 and 4

Note that despite the independent nature of congestion patterns over US 50's segments 3 and 4, their traffic queues during peak periods (due to rapid propagation and spillback) often evolve backward to integrate with one oversaturated traffic pattern over US 50 (see Figure 4-

14), mostly occurring around 11am on weekends in the summer season. Hence, to prevent such complete roadway blockage one shall deploy two traffic sensors (i.e., at C16 and C17) between these two congested segments to detect spatial evolution of their traffic queues and take timely control strategies to prevent the formation of traffic breakdown. The geometric feature of the two locations for deploying traffic sensors are shown in Figure 4-15.



Figure 4-14: geometric features of the two locations (C16 and C17) for detector placement



- Traffic flow monitoring
- ▲ Identifying congestion patterns and spillovers
- ◆ Existing infrastructure

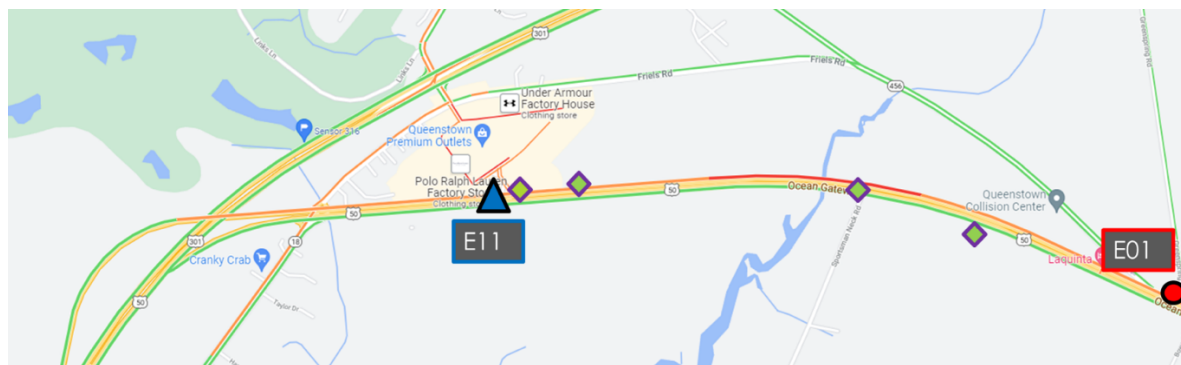
NO.	LOCATION	LOCATION TYPE	NEARBY POLES?	PRIORITY
C16	38.840113, -76.060447	Roadside	Yes	Required
C17	38.905438, -76.061768	Roadside	No	Desired

Figure 4-15: List of detectors recommended for Cluster 5 congested highway segment in the Eastern Shore region

Cluster 6 congested highway segment

Different from other congested segments, the formation of congestion queues along US 50 around Queenstown is mainly because of traffic to-and-from the nearby premium business outlet. The weaving movements from merging in and out of a high volume highway naturally contribute to the speed reduction and formation of traffic shockwaves, which will inevitably propagate congestion to its upstream segment. Hence, for monitoring such traffic queue propagation patterns, it is suggested that a detector be placed at location E01 (see Figure 4-16). One may also consider deploying one detector at the intersection (i.e., E11) to monitor traffic to-and-from the premium outlet, so that the signal control can be so designed to balance the needs between US 50's mainline flows from upstream and its merging traffic from the roadside entry.

Recommended sensor locations



- Traffic flow monitoring
- ▲ Identifying congestion patterns and spillovers
- ◆ Existing infrastructure

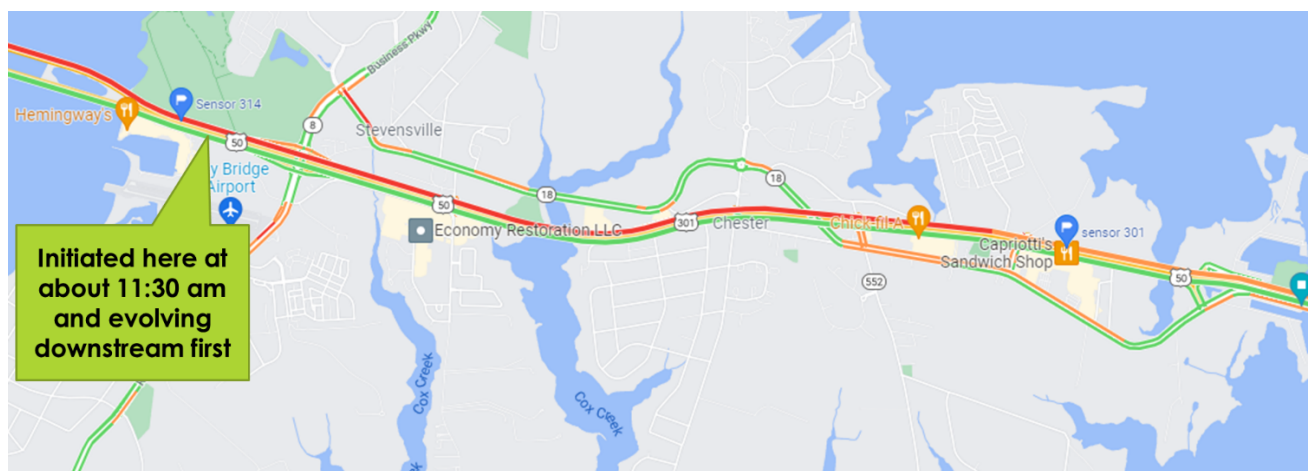
NO.	LOCATION	LOCATION TYPE	NEARBY POLES?	PRIORITY
E01	38.980320, -76.141082	Roadside	No	Required
E11	38.981851, -76.159154	Intersection	Yes	Desired

Figure 4-16: List of detectors recommended for Cluster 6 congested highway segment in the Eastern Shore region

Cluster 7 congested highway segment: US 50 segment over Kent Island

As shown in Figure 4-17, this segment of US 50 suffers the worst congestion in the Eastern Shore region due to the heavy local traffic moving in and out from Kent Island, which typically sustains more than eight hours of congestion during the peak travel season. Traffic streams contributing to the congestion come not only from the mainline upstream, but also multiple contributors such as local intersection flows, vehicles from Kent Island that merge on to US 50, and tourists getting off US 50 for a Kent Island local tour. Hence, eight detectors are recommended for traffic control needs in this area, if the budget for deployment is not a constraint. Among those, detector F01 is for intersection traffic monitoring, and detectors F11, F13, and F14 shall be a priority for deployment if one intends to implement any traffic control strategy to mitigate the congestion in this area.

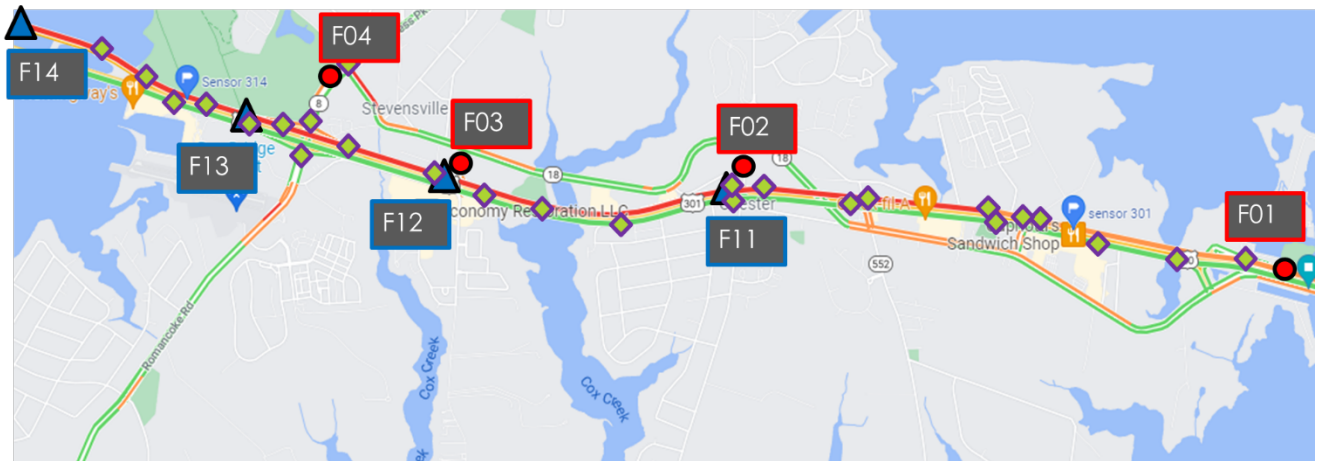
Figure 4-18 displays the list of locations for detectors for either traffic monitoring or congestion control. Five candidate locations, which have nearby roadside signal poles for mounting traffic sensors, are also listed in the figure.



Congestion pattern
1 pm - 9 pm
Evolves upstream
Significantly impacts local traffic

Figure 4-17: Results of congestion pattern analysis for Cluster 7 congested highway segment in the Eastern Shore region

Recommended sensor locations



- Traffic flow monitoring
- ▲ Identifying congestion patterns and spillovers
- ◆ Existing infrastructure

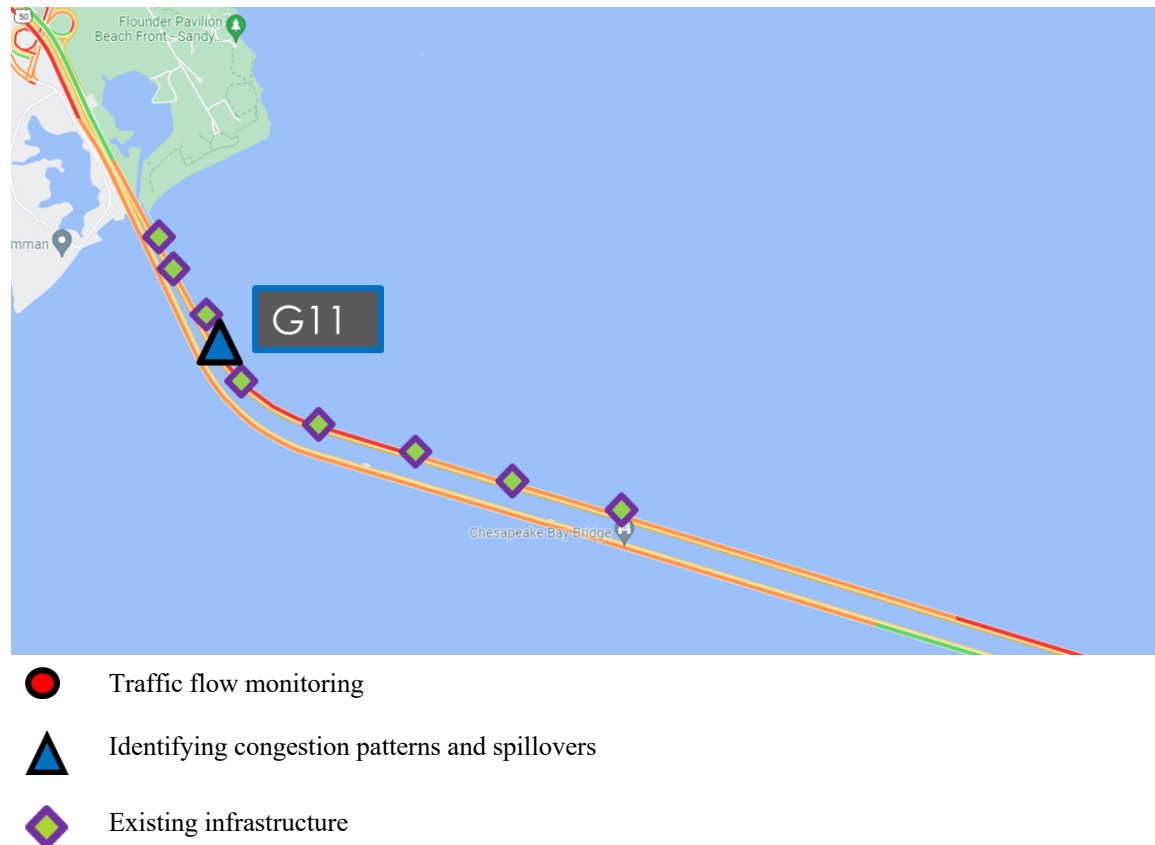
NO.	LOCATION	LOCATION TYPE	NEARBY POLES?	PRIORITY
F01	38.972021, -76.252337	Roadside	Yes	Required
F02	38.976659, -76.289757	Roadside	No	Optional
F03	38.977247, -76.310395	Roadside	No	Optional
F04	38.982127, -76.320117	Roadside	No	Optional
F11	38.975967, -76.291331	On-ramp	Yes	Desired
F12	38.976912, -76.312183	On-ramp	Yes	Optional
F13	38.980384, -76.326738	On-ramp	Yes	Desired
F14	38.985118, -76.342110	On-ramp	Yes	Desired

Figure 4-18: List of detectors recommended for Cluster 7 congested highway segment in the Eastern Shore region

Cluster 8 congested highway segment: Bay Bridge

Figure 4-19 displays the congestion pattern on the US 50 segment over the Bay Bridge, which is due mainly to the high entry volume and the expected capacity reduction over the bridge segment. Its congested period is identical to that in the Kent Island area. Since there exists no entry and exit over the bridge segment, deploying one detector will be sufficient for either monitoring traffic conditions or implementing time-varying speed control.

Recommended congestion locations



NO.	LOCATION	LOCATION TYPE	NEARBY POLES?	PRIORITY
G11	38.999474, -76.397187	Bridge	Yes	Desired

Figure 4-19: List of detectors recommended for Cluster 8 congested highway segment over Bay Bridge

4.4 Summary Findings

This chapter has first presented a systemic process for identifying candidate locations for detector deployment, and then summarized its application results for the Eastern Shore region. The proposed process considers the detectable traffic streams, congestion patterns,

and available infrastructure for mounting sensors. Table 4-1 presents the application results of the proposed sensor location selection process, where all identified locations for sensor deployment, based on the purpose of applications, are classified into the following three sets: traffic monitoring only, congestion pattern identification, and traffic controls and congestion mitigation. Responsible traffic engineers can then set the deployment priority based on the available budget and intended applications.

Note that the proposed process for sensor location selection is generic in nature, so it is applicable to other regions without using complex mathematical programs for optimal location selection.

Table 4-1 Summary of detector locations recommended for Eastern Shore deployment.

Number	Location	Total recommended number of sensors	Number of required/desired sensor locations	Number of required/desired sensors that can be deployed at the existing infrastructure
1	OC drawbridge	5	3	3
2	Cambridge	8	4	3
3	Easton	10	4	4
4	MD 404 & MD 213	7	7	2
3 & 4	North of Easton	2	2	1
5	US 301	2	2	1
6	Kent Island	8	4	4
7	Bay Bridge	1	1	1

Chapter 5: Conclusion and Recommendations

5.1 Conclusion of Research Findings

This study has addressed three major tasks and offered results for field deployments. The first is to design a set of guidelines for selecting the deployment locations for traffic sensors in the Easter Shore region for different purposes, such as speed monitoring, signal design, or congestion control. Accounting for the tradeoff between the spatial coverage of detectors and the available traffic information, the developed guidelines allow the potential users to prioritize candidate locations for deploying traffic sensors and to design the optimal deployment plan under existing funding constraints and selected traffic management strategies for the region.

The second accomplishment of this study is to design an innovative, multi-stage control model for traffic professionals to efficiently assess the quality of massive speed and flow rate data produced from a deployed detector. Based on the quality assessment results, the responsible maintenance engineers/staff can better classify the operational status of each deployed detector, including “for speed-monitoring only,” “for traffic control and management,” “need to replace with new detector,” and “need a field calibration to improve the detection accuracy.” The entire quality assessment process starts with either on-line or off-line computation of a missing data rate over the per-specified time span. It is followed by executing a set of validity tests with respect to the percentage of data falling into a set of reasonable upper and lower bounds, which are pre-calibrated with the information from the historical traffic patterns, roadway geometric constraints, and feasible ranges of the detector’s measurements, such as the maximum speed and flow rate.

The last and most critical stage of the data quality assessment is to evaluate the speed and flow data, passing through the Stage 1 screening process, with three sequential speed-flow relationship tests to ensure that the detector’s traffic measurements are consistent with the aggregated speed-flow patterns identified in the traffic flow theory, and also distinctly reflect the time-of-day traffic conditions under different congestion levels. Based on the percentage of data passing through the last speed-flow relationship tests, responsible traffic engineers can then decide if the target detector’s key detection parameters must be recalibrated, or if its produced traffic measurements are sufficiently reliable for design of various traffic management plans or control strategies.

For convenience of using the detector quality assessment model, this study has further converted its embedded, multi-stage screening process into an interactive and user-friendly computer program for either on-line or off-line execution. This computer program, along with its supplemental module to illustrate a radar detector’s field calibration procedure, will enable

the maintenance staff/engineers to efficiently identify which traffic detectors cannot yield sufficiently reliable data for traffic monitoring or other target applications.

5.2 Potential Extensions

Although the developed multi-stage assessment model has demonstrated its effectiveness with respect to existing radar sensors in the Eastern Shore region, it is imperative that the following refinement tasks be rigorously conducted to ensure its reliable performance to other highway networks of different geometric features, congestion, patterns, and driving populations:

- Recalibrate the model's Stage 2 screening parameters—such as the maximum speed and flow rate during peak and off-peak periods for validity tests—using the target highway's historical time-of-day traffic characteristics data.
- Perform extensive sensitivity tests to evaluate the impacts of major changes in roadway geometric features (e.g., lane-closure, on-ramp weavings) on the robustness of the model's Stage 2 parameters and construct a set of such parameters for different target highways if needed.
- Develop an effective transferability process for updating the multi-stage quality assessment model's Stage 2 screening parameters and control thresholds.

The speed-flow data for the model development and calibration of speed-flow relations are from a well-calibrated detector in the Eastern Shore region, although the primary relationships between traffic flow rates and speeds should exhibit the same pattern, regardless of the available travel lanes. However, its traffic measurement data—reflecting the complex interactions of driving populations under different geometric and congestion environments—may exhibit a distribution of higher variance than that from a two-lane highway (which make up most of the Eastern Shore region) in the fundamental speed-flow diagram. Hence, to ensure the effectiveness of the developed detector assessment model's applications to other highways, one shall first perform its transferability evaluation with key information from the target highway, and then design a convenient parameter update procedure to ensure its performance robustness.

- Develop a transferability data bank for potential users to select the set of optimal screening/control parameters for best use of the detector quality assessment model, based on the key characteristics and information associated with the target highway networks and their primary driving populations (e.g., commuters or tourists).

As for extending the detector deployment guide for the Eastern Shore region for other

highway networks, one shall first conduct the following enhancement tasks:

- Develop the guidelines for identifying candidate locations for potential deployment of radar-based traffic sensors, including the radar-zone coverage constraints and geometric features that are essential for executing the detection functions.
- Incorporate the spatial distribution of congestion patterns over a highway network and the budget constraints per deployment phase in design of the sensor deployment guide so that the users can effectively prioritize the list of locations for deploying traffic sensors.
- Extend the operational guide for traffic sensors deployed for different purposes, such as speed/volume monitoring, congestion control, or signal design.

In summary, with the above enhancements the entire detector deployment guide shall comprise the following three major parts: selection of candidate locations sensor deployment, the optimized sequential deployment plan under the resource constraints, and detector quality assessment program for performance evaluation. Highway agencies can certainly take advantage of such a tool and guide for best planning their traffic surveillance systems and performing essential sensor quality assessment in a timely manner.

References

- Ametha, J., Turner, S., & Darbha, S. 2001. Formulation of a new methodology to identify erroneous paired loop detectors. IEEE Intelligent Transportation Systems. Proceedings (Cat. No. 01TH8585) pp. 591-596.
- Al-Deek, H. M., Venkata, C., & Chandra, S. R. 2004. New algorithms for filtering and imputation of real-time and archived dual-loop detector data in I-4 data warehouse. Transportation research record, *1867*(1), pp. 116-126.
- Azin, B. and Yang, X. T. 2020. Multi-Stage Algorithm for Detection-Error Identification and Data Screening (No. UT-20.15). Utah. Dept. of Transportation. Research Division.
- Arianezhad, A., & Wu, Y. J. 2020. Large-scale loop detector troubleshooting using clustering and association rule mining. Journal of Transportation Engineering, Part A: Systems, *146*(7), 04020064.
- Brian, L. S., Ramkumar V. 2003. ITS data quality: Assessment procedure for freeway point detectors (Virginia Transportation Research Council)
- Brilon, W. and Lohoff, J. 2011. Speed-flow Models for Freeways. In 6th International Symposium on Highway Capacity and Quality Service, Stockholm, Sweden, Jun. *16*, pp. 26-36.
- Chen, L. and May, A. D. 1987. Traffic detector errors and diagnostics. Transportation research record, *1132*, pp. 82-93.
- Cleghorn, D., Hall, F.L. & Garbuio, D. 1991. Improved data screening techniques for freeway traffic management systems. Transportation Research Record, *1320*(1320-1324), pp. 17-23
- Coifman, B. 1999. Using dual loop speed traps to identify detector errors. Transportation Research Record, *1683*(1), pp. 47-58.
- Chen, C., Kwon, J., Rice, J., Skabardonis, A., & Varaiya, P. 2003. Detecting errors and imputing missing data for single-loop surveillance systems. Transportation Research Record, *1855*(1), pp. 160-167.
- Coifman, B. and Dhoorjaty, S. 2004. Event data-based traffic detector validation tests. Journal of Transportation Engineering, *130*(3), pp. 313-321.
- Corey, J., Lao, Y., Wu, Y. J., & Wang, Y. 2011. Detection and correction of inductive loop detector sensitivity errors by using gaussian mixture models. Transportation Research Record, *2256*(1), pp. 120-129.

- Chen, Z., Qin, X., Schneider, E., Cheng, Y., Parker, S. & Shaon, R.R. 2019. Designing a comprehensive procedure for flagging archived traffic data: A case study. *Transportation Research Record*, 2673(6), pp. 165-175.
- Dowling, R., Skabardonis, A., & Alexiadis, V. 2004. Traffic analysis toolbox, volume III: Guidelines for applying traffic microsimulation modeling software (No. FHWA-HRT-04-040). United States. Federal Highway Administration (FHWA). Office of Operations
- Electronic Integrated Systems Inc., “RTMS Side Fired Training.”
- Ghafouri, A., Laszka, A., Dubey, A., & Koutsoukos, X. 2017. Optimal detection of faulty traffic sensors used in route planning. In *Proceedings of the 2nd international workshop on science of smart city operations and platforms engineering*, pp. 1-6.
- Huber, G., Bogenberger, K., & Bertini, R. L. 2014. New Methods for Quality Assessment of Real Time Traffic Information. *Transport Research Board 93rd. Annual Meeting*.
- Ishak, S., Kondagari, S., & Alecsandru, C. 2007. Probabilistic data-driven approach for real-time screening of freeway traffic data. *Transportation Research Record*, 2012(1), pp. 94-104.
- Jacobson, L. N., Nihan, N. L., & Bender, J. D. 1990. Detecting erroneous loop detector data in a freeway traffic management system. *Transportation Research Record*, 1287, pp. 151-166
- Lu, Y., Yang, X. & Chang, G.-L. 2014. Algorithm for detector-error screening on basis of temporal and spatial information. *Transportation Research Record* 2443(1), pp. 40-48
- MacQueen, J. 1967. Classification and analysis of multivariate observations. In *5th Berkeley Symp. Math. Statist. Probability*, pp. 281-297.
- McLachlan, G., *Mixture Models*, New York, NY, USA:Marcel Dekker, 1988.
- Nihan, N. L. 1990. *Detector Data Validity*. Publication WA-RD208.1. Washington State Department of Transportation
- Peeta, S. and Anastassopoulos, I. 2002. Automatic real-time detection and correction of erroneous detector data with fourier transforms for online traffic control architectures. *Transportation Research Record*, 1811(02-2244), pp. 1-11.
- Rousseeuw, P. J., Ruts, I., & Tukey, J. W. 1999. The bagplot: a bivariate boxplot. *The American Statistician*, 53(4), pp. 382-387
- Seddon, P. A. 1971. Another Look at Platoon Dispersion: 1. The Kinematic Wave Theory. *Traffic Engineering and Control*, pp. 332–336.

- Smith, B. L., and Venkatanarayana, R. 2007. New methodology for customizing quality assessment techniques for traffic data archives. *Transportation Research Record*, 1993(1), pp. 165-174
- Tukey, J. W. 1975. Mathematics and the picturing of data. In *Proceedings of the International Congress of Mathematicians, Vancouver. 2*, pp. 523-531.
- Turochy, R. E. and Smith, B. L. 2000. New procedure for detector data screening in traffic management systems. *Transportation Research Record*, 1727(1), pp. 127-131.
- Turner, S., Albert, L., Gajewski, B., & Eisele, W. 2000. Archived intelligent transportation system data quality: Preliminary analyses of San Antonio TransGuide data. *Transportation Research Record*, 1719(1), pp. 77-84.
- Truong, C., Oudre, L., & Vayatis, N. 2020. Selective review of offline change point detection methods. *Signal Processing*, 167, 107299.
- Underwood, R.T. 1961. Speed, volume and density relationships. In: *Quality and Theory of Traffic Flow*; Bureau of Highway Traffic, Yale University, New Haven; pp. 141-187.
- Vanajakshi, L., & Rilett, L. R. (2004). Loop detector data diagnostics based on conservation-of-vehicles principle. *Transportation Research Record*, 1870(1), 162-169.
- Wall, Z. R., and Dailey, D. J. 2003. Algorithm for detecting and correcting errors in archived traffic data. *Transportation Research Record*, 1855(1), pp. 183-190.
- Weijermars, W. A. and Van Berkum, E. C. 2006. Detection of invalid loop detector data in urban areas. *Transportation Research Record*, 1945(1), pp. 82-88.
- Wang, Y., Corey, J., Lao, Y., & Wu, Y. J. 2009. Development of a statewide online system for traffic data quality control and sharing (No. TNW2009-12). *Transportation Northwest (Organization)*.
- Wu, Y. J., Zhang, G., & Wang, Y. 2010. Volume data correction for single-channel advance loop detectors at signalized intersections. *Transportation Research Record*, 2160(1), pp. 128-139.
- Wavetronix LLC. 2018. Documentation 0299- How Does the SmartSensor HD Measure Occupancy?
- Zefreh, M. M., & Torok, A. 2018. Single loop detector data validation and imputation of missing data. *Measurement*, 116, pp. 193-198.

Appendices

Appendix-A

Figure A-1 shows the detailed analysis results that can be downloaded for more information from the developed software.

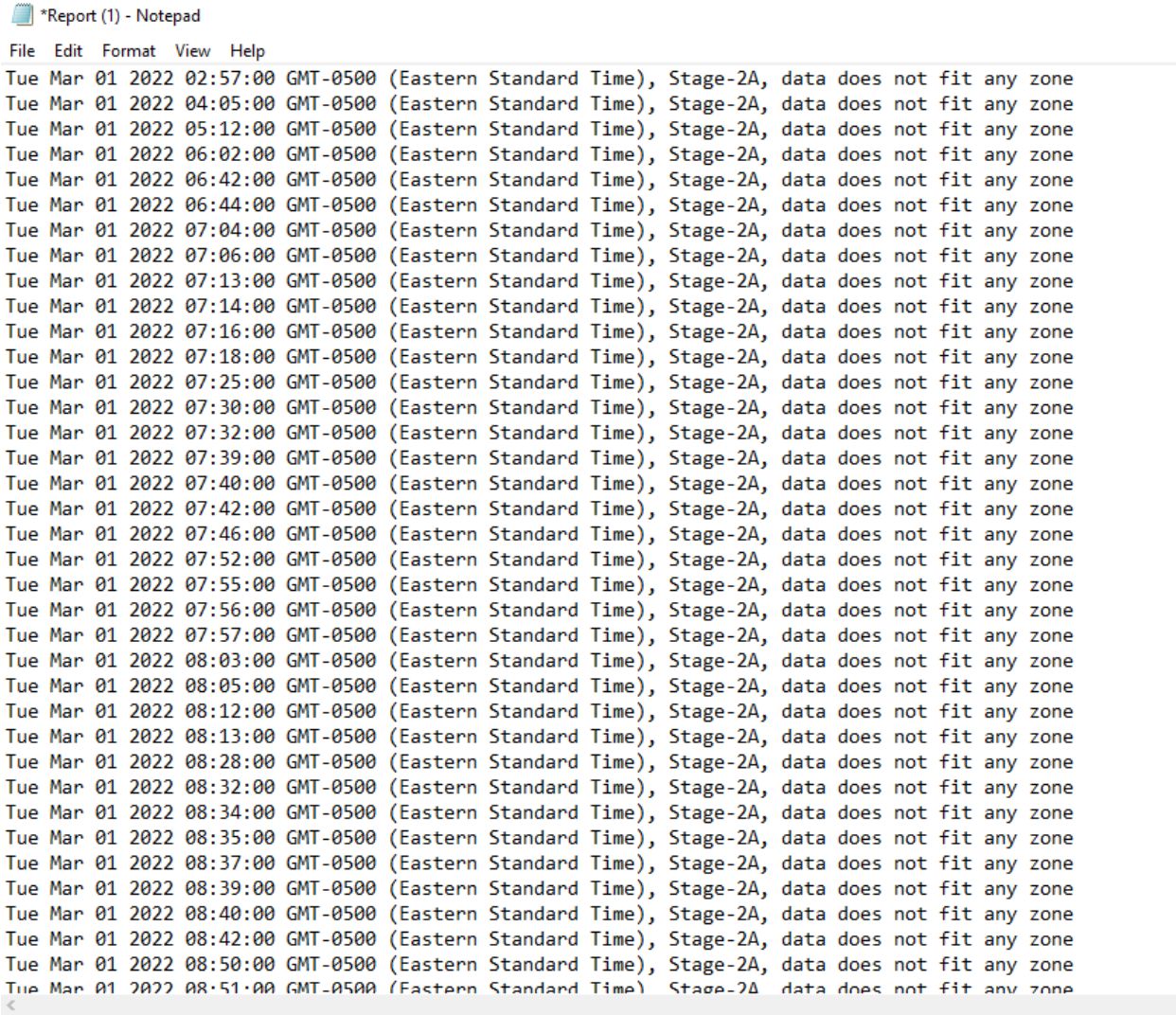


Figure A-1: An example of the downloaded analysis results from the developed software

Appendix-B

Sensor Accuracy Evaluation Results

Reported by Applied Technology and Traffic Analysis Program (ATTAP) and Traffic Safety and Operations Lab in University of Maryland – College Park

Evaluation Method

- Data collection tool: Unmanned Ariel Vehicle (UAV), i.e., drones
 - Data processing platform: RCE systmes s.r.o (2022)
- Data Collection Date
 - 04/22/2022: S122001, S122002, S217004, S217002, S217003
 - 04/29/2022: S110002, S110001, S110003
- Data Collection Duration
 - One hour for each location

Evaluation Results

All sensors can produce reliable measurements, as presented in Table 1, for traffic monitoring, planning, and control operations. One exception: Lane 3 of sensor S217004 may need to be recalibrated for its radar wave coverage, because it seems to be impacted by the presence of the roadway median.

Table B-1: Evaluation results of sensor accuracy

Sensor	Lane#	Volume (1 min) ¹	Volume (15 min)	Volume (60 min)	Speed (1 min) ²	Speed (15 min)	Speed (60 min)
S122001	Lane1	7.3%	3.5%	3.6%	1.6%	0.2%	0.1%
	Lane2	1.0%	1.0%	1.0%	0.8%	0.4%	0.4%
S122002	Lane1	5.9%	2.4%	1.5%	0.7%	0.4%	0.1%
	Lane2	2.2%	0.3%	0.2%	1.0%	0.4%	0.3%
S217004	Lane1	4.6%	0.6%	0.0%	1.2%	0.5%	0.4%
	Lane2	4.2%	1.8%	1.7%	1.1%	0.8%	0.2%
	Lane3	18.9%	12.5%	12.3%	1.6%	0.4%	0.1%
	Lane4	4.4%	2.8%	1.6%	1.5%	0.4%	0.2%
S217002	Lane1	0.0%	0.0%	0.0%	0.4%	0.2%	0.2%
	Lane2	1.0%	0.9%	0.2%	0.5%	0.4%	0.2%
S217003	Lane1	1.8%	1.0%	0.8%	0.8%	0.2%	0.1%
	Lane2	2.5%	1.0%	0.4%	0.8%	0.3%	0.3%
	Lane3	1.0%	1.0%	1.0%	0.9%	0.8%	0.2%
	Lane4	2.8%	1.5%	0.0%	1.0%	0.4%	0.4%
	Lane5	1.6%	0.3%	0.2%	0.7%	0.2%	0.0%
	Lane6	0.0%	0.0%	0.0%	0.7%	0.4%	0.3%
S110002	Lane1	1.4%	1.2%	0.7%	0.8%	0.4%	0.3%
	Lane2	3.4%	2.9%	2.2%	1.1%	0.5%	0.5%
	Lane3	1.1%	0.5%	0.0%	1.3%	0.5%	0.4%
	Lane4	3.1%	1.7%	0.0%	1.3%	0.6%	0.5%
S110001	Zone1 ³	1.5%	0.4%	0.0%	0.6%	0.3%	0.0%
	Lane3	4.2%	2.2%	0.7%	0.6%	0.1%	0.0%
	Lane4	2.1%	1.8%	1.8%	1.2%	0.6%	0.2%
S110003	Lane1	1.5%	0.4%	0.0%	0.6%	0.3%	0.0%
	Lane2	4.2%	2.2%	0.7%	0.6%	0.1%	0.0%

Note:

¹ Volume (1 min) represents the average rate of volume difference (%), aggregated in 1 minute, between the data collected from roadside sensor and drones

² Speed (1 min) represents the average rate of speed difference (%), aggregated in 1 minute, between the data collected from roadside sensor and drones

³ Westbound of sensor S110001 involves two lanes to one lane merging, thus the westbound traffic is evaluated by considering two lanes together.

For the lane configuration of each sensor, one can refer to the following figures.



Figure B-1: Lane configuration Sensor S122001

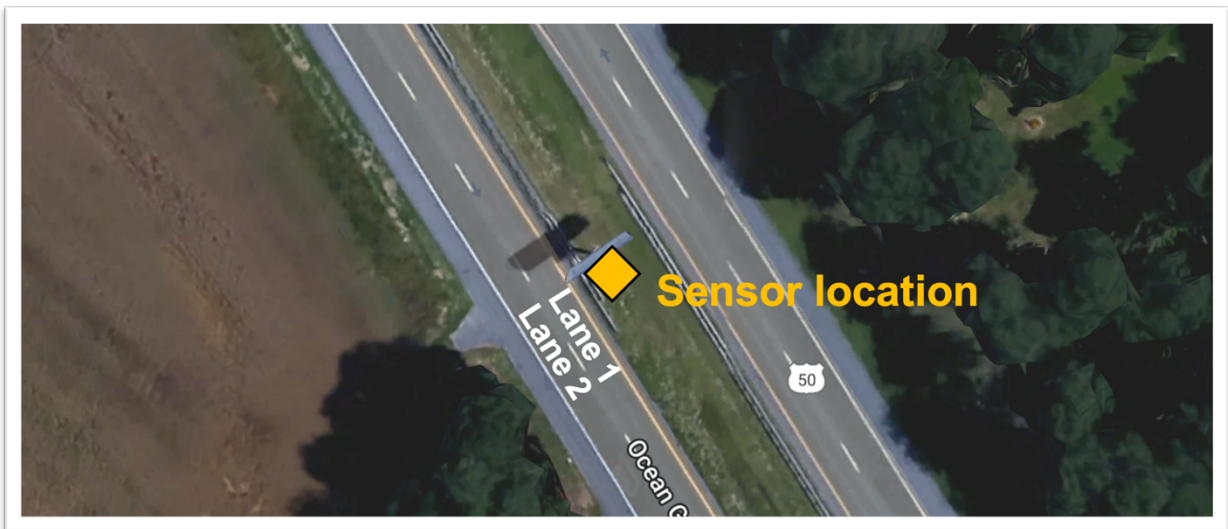


Figure B-2: Lane configuration Sensor S122002



Figure B-3: Lane configuration Sensor S217004



Figure B-4: Lane configuration Sensor S217002



Figure B-5: Lane configuration Sensor S217003



Figure B-6: Lane configuration Sensor S110002



Figure B-7: Lane configuration Sensor S110001



Figure B-8: Lane configuration Sensor S110003